A novel Ca^{2+}-mediated cross-talk between endoplasmic reticulum and acidic organelles: implications for NAADP-dependent Ca^{2+} signalling

Duilio Michele Potenza[a,f], Virginia Ronco[b,f], Federico Denti[a], Sabrina Vullo[a], Giuseppe Gagliano[a], Marialuisa Tognolina[c], Germano Guerra[d], Paolo Pinton[e], Armando A. Genazzani[b], Lisa Mapelli[c], Francesco Moccia[a,*], and Dmitry Lim[b,*]

[a]Laboratory of Physiology, Department of Biology and Biotechnology "Lazzaro Spallanzani", University of Pavia, 27100 Pavia, Italy;
[b]Department of Pharmaceutical Sciences, University of Eastern Piedmont "Amedeo Avogadro", 28100 Novara, Italy;
[c]Laboratory of Neurophysiology, Department of Brain and Behavioural Sciences, University of Pavia, 27100 Pavia, Italy;
[d]Department of Medicine and Health Sciences, University of Molise, 86100 Campobasso;
[e]Department of Morphology, Surgery and Experimental Medicine, Section of Pathology, Oncology and Experimental Biology, Laboratory for Technologies of Advanced Therapies (LTTA), University of Ferrara, 44121 Ferrara, Italy;
[f]These authors equally contributed to the work and share First Authorship;
*these authors should be considered as co-last authors and share Senior Authorship.

* Corresponding authors:
Dr. Francesco Moccia
Laboratory of General Physiology,
Department of Biology and Biotechnology "Lazzaro Spallanzani",
University of Pavia,
Via Forlanini 6, 27100 Pavia, Italy.
Tel: 0039 0382 987169
Fax: 0039 0382 987527
E-mail: francesco.moccia@unipv.it

And

Dr. Dmitry Lim
Department of Pharmaceutical Sciences,
University of Eastern Piedmont "Amedeo Avogadro",
Via Bovio 6, 28100 Novara, Italy
Tel: 0039 0321 375827
Fax: 0039 0321 375821
E-mail: dmitry.lim@pharm.unipmn.it

Running title: Ca^{2+}-mediated ER-lysosome interaction and NAADP signalling

Authors' email addresses:

Duilio Michele Potenza: duiliomichele@hotmail.it
Virginia Ronco: virginia.ronco@pharm.unipmn.it
Federico Denti: fdenti@sund.ku.dk
Sabrina Vullo: sabrinavullo@tiscali.it
Giuseppe Gagliano: giuseppe.gagliano90@gmail.com
Marialuisa Tognolina: marialuisa.tognolina01@ateneopv.it
Germano Guerra: germano.guerra@unimol.it
Paolo Pinton: pnp@unife.it
Armando Genazzani: armando.genazzani@pharm.unipmn.it
Lisa Mapelli: lisa.mapelli@unipv.it
Francesco Moccia: francesco.moccia@unipv.it
Dmitry Lim: dmitry.lim@pharm.unipmn.it

Abstract

Nicotinic acid adenine dinucleotide phosphate (NAADP) serves as the ideal trigger of spatio-temporally complex intracellular Ca^{2+} signals. However, the identity of the intracellular Ca^{2+} store(s) recruited by NAADP, which may include either the endolysosomal (EL) or the endoplasmic reticulum (ER) Ca^{2+} pools, is still elusive. Here, we show that the Ca^{2+} response to NAADP was suppressed by interfering with either EL or ER Ca^{2+} sequestration. The measurement of EL and ER Ca^{2+} levels by using selectively targeted aequorin unveiled that the preventing ER Ca^{2+} storage also affected ER Ca^{2+} loading and *viceversa*. This indicates that a functional Ca^{2+}-mediated cross-talk exists at the EL-ER interface and exerts profound implications for the study of NAADP-induced Ca^{2+} signals. Extreme caution is warranted when dissecting NAADP targets by pharmacologically inhibiting EL and/or the ER Ca^{2+} pools. Moreover, Ca^{2+} transfer between these compartments might be essential to regulate vital Ca^{2+}-dependent processes in both organelles.

Introduction

Nicotinic acid adenine dinucleotide phosphate (NAADP) represents the latest addition to the restricted family of intracellular Ca^{2+}-releasing messengers [1], already including inositol-1,4,5-trisphosphate and cyclic ADP-ribose (cADPr). NAADP may be synthesized upon cellular stimulation or activation of cell surface receptors to regulate a plethora of intracellular processes, including fertilization [2, 3], muscle contraction [4], nitric oxide (NO) production [5], and glucose metabolism [6]. Its efficacy in triggering cytosolic Ca^{2+} elevations, as compared to either $InsP_3$ or cADPr, is underscored by the low doses of NAADP required to activate cell signalling, spanning from pM to low nM concentrations [7]. While $InsP_3$ and cADPr have long been known to mobilize Ca^{2+} from endoplasmic reticulum (ER), by activating $InsP_3$ ($InsP_3Rs$) and ryanodine (RyRs) receptors [8], respectively, the molecular target of NAADP has been far more elusive. Pioneering work conducted on sea urchin egg homogenates demonstrated that the NAADP-sensitive Ca^{2+} store is physically and pharmacologically separated from that recruited by $InsP_3$ and cADPr [9, 10]. Consistent with this observation, NAADP was later found to discharge Ca^{2+} from acidic lysosome-like organelles in sea urchin eggs [11], where the newly discovered family of two-pore channels (TPCs) serve as the long-sought NAADP receptors [9, 12]. However, this mechanism does not underlie NAADP-mediated Ca^{2+} signalling in the closely related starfish oocytes; herein, NAADP does not mobilize Ca^{2+} from acidic Ca^{2+} stores [13], but activates a plasmalemmal inwardly-rectifying Ca^{2+} permeable channel [14, 15]. Subsequent work has shown that NAADP may release Ca^{2+} from acidic organelles of the endolysosomal (EL) system, which include early, late and recycling endosomes, in mammal cells: TPCs mediate a trigger Ca^{2+} release that is amplified into a regenerative Ca^{2+} wave by the Ca^{2+}-dependent recruitment of RyRs and/or $InsP_3Rs$ [7, 9]. Alternatively, NAADP may gate TPCs to shuttle EL Ca^{2+} into ER by stimulating Sarco-Endoplasmic Reticulum Ca^{2+}-ATPase (SERCA) activity, thereby promoting further Ca^{2+} liberation via either $InsP_3Rs$ and/or RyRs [4, 16, 17]. This model has been challenged by several observations, according to which RyRs type 1 and 2 (RyR1 and RyRs2) may serve as primary target for NAADP both in naïve cells and in planar lipid bilayers [18-20]. The debate around the primary site of action of NAADP remains therefore, highly controversial [18, 21-23]. Whereas gene silencing experiments have demonstrated TPC contribution to NAADP-evoked Ca^{2+} signals, the involvement of acidic organelles has been mainly supported by the use of pharmacological tools [7, 9, 24, 25]. A number of drugs have been utilized to either disrupt or interfere with lysosome acidification, thereby disrupting their Ca^{2+} storage ability and preventing the Ca^{2+} response to NAADP. These compounds include: glycyl-L-phenylalanine-2-naphthylamide (GPN), a substrate of lysosomal

cathepsin C whose cleavage causes osmotic lysis of lysosomes; bafilomycin A1, a highly selective inhibitor of V-type H^+-ATPase that drives the proton gradient responsible for Ca^{2+} sequestration; and nigericin, a H^+/K^+ ionophore which dissipates the proton gradient across lysosome membrane [9, 24-26]. A recent series of studies have disclosed the tight and finely tuned inter-organellar communication that occurs during intracellular Ca^{2+} movement between EL and ER compartments and *viceversa* [27-31]. In this regard, only a few studies have assessed whether the pharmacological disruption of acidic Ca^{2+} stores affects ER Ca^{2+} loading [27, 29, 32-34], thereby inadvertently masking its participation to the onset and development of NAADP-evoked Ca^{2+} signals. In turn, there is scant information about the consequences of ER SERCA blockade by thapsigargin, cyclopiazonic acid (CPA) and and 2,5-di-(t-butyl)-1,4-hydroquinone (TBHQ) on the Ca^{2+} content of acidic stores [24, 25, 33].

The present investigation was endeavoured to first dissect the intracellular Ca^{2+} stores responsible for NAADP-induced Ca^{2+} release in HeLa cells, a widely employed cell model to study intracellular Ca^{2+} signalling. This step was essential to then unveil: 1) whether and how the pharmacological manipulation of the EL Ca^{2+} pool impairs ER Ca^{2+} levels and *viceversa* and 2) to ascertain the implications of the ER-EL Ca^{2+} movements for NAADP-induced Ca^{2+} signals. We took benefit from "whole-cell patch-clamp" recordings to dyalize NAADP into the cytosol and monitor the activation of a Ca^{2+}-dependent membrane current as surrogate of the concomitant intracellular Ca^{2+} response [35-37]. Additionally, we used aequorin-based Ca^{2+} probes to assess the effects of GPN, bafilomycin A1, nigericin, and thapsigargin on both ER and EL Ca^{2+} loading. Our data provide further support to the trigger hypothesis, whereby NAADP engages TPCs to discharge a local bolus of Ca^{2+} which is in turn amplified by adjoining RyRs and $InsP_3Rs$. However, we further demonstrated that a functional Ca^{2+}-mediated cross-talk does occur between EL and ER Ca^{2+} stores to reciprocally control their refilling. It turns out that the pharmacological manipulation of acidic organelles may exert profound consequences on the extent of ER Ca^{2+} storage and *viceversa*; this feature should be taken in account when investigating the primary target of NAADP in mammal cells.

Materials and Methods

Cell cultures

HeLa cells were cultured in DMEM (Sigma) medium supplemented with 10% FBS (Immunological Sciences), 2 mM glutamine and 1% penicillin streptomycin (Sigma) in humidified atmosphere containing 5% CO_2. Cells were grown to 80% confluence and passaged twice a week. For experiments the cells were plated onto glass coverslips at concentrations $5x10^4$ per ml (24 mm diameter coverslips in 6 well plates) or $3x10^4$ per ml (13 mm diameter coverslips in 24 well plates).

Electrophysiological recordings

Membrane currents were recorded from isolated HeLa cells (3 days in culture) by using the conventional whole cell patch-clamp configuration and a L/M EPC-7 patch-clamp amplifier (List-Electronic; Darmstadt, Germany) [38]. Whole cell currents were sampled at 1 kHz and acquired by exploiting the Strathclyde electrophysiology software WinWCP (courtesy of Dr. John Dempster, University of Strathclyde, Glasgow UK). Alternatively, they were recorded by using a Multiclamp 700B amplifier (−3dB; cut-off frequency = 10 kHz) driven by PClamp 10 software (Molecular Devices, Union City, CA, USA). Pipettes were pulled from thin-walled borosilicate glass using a Sutter Instruments P-87 pipette puller and had resistances of 3-5 MΩ when filled with high-K^+ internal solution. Patch pipettes were pulled from borosilicate glass capillaries (Warner Instruments Corp., Hamden, CT, USA) and filled with the following solution: KCl (140 mM), NaCl (8 mM), $MgCl_2$ (1.5 mM), HEPES (10 mM), EGTA (0.05 mM), titrated to pH=7.2 with KOH. NAADP was added at the final concentration of 10 nM, otherwise stated. In order to assess the Ca^{2+}-sensitivity of NAADP-evoked currents, EGTA was added at a final concentration of 10 mM. Cells were maintained in a standard physiological salt solution [38]: NaCl (150 mM), KCl (6 mM), $MgCl_2$ (1 mM), $CaCl_2$ (1.5 mM), HEPES (10 mM), glucose (10 mM) adjusted to pH=7.4 with NaOH. Access resistances were <10 MΩ following series resistance compensation. Current-voltage (I-V) curves were obtained by applying, every 1 s, 100 ms voltage ramps ranging from -100 mV to + 100 mV and delivered from a holding potential of 0 mV [39]. Currents were normalised by dividing the amplitudes (measured from the voltage ramps at −80 mV and +80 mV) by the cell capacitance. Capacitative currents were compensated before each ramp by using the amplifier's built-in compensation section. All leak currents were subtracted by averaging the first two to ten ramp currents, and then subtracting this from all subsequent currents. Pooled data are given as mean±Se and statistical evaluation was carried out using Student's unpaired T test. Experiments were carried out at room temperature (20–23°C).

Generation of CathD-Aeq Ca^{2+} probe and aequorin Ca^{2+} measurements

CathD-Aeq and ER-Aeq aequorin-based Ca^{2+} sensors were used to measure the rate of Ca^{2+} uptake and the steady-state Ca^{2+} levels in the endo-lysosomal organelles (EL) and in the ER, respectively. The ER-Aeq Ca^{2+} probe was described in [40]. For generation of the CathD-Aeq Ca^{2+} probe a fragment of the the cathepsin D (CathD) cDNA was first amplified using the following primers: Forward: 5'- ggaagcttgaattcgccaccatgcagccctccag -3' Reverse: 5'-ggaagcttgagggtcttcccggcctgcgacacct -3' which caused the addition of a HindIII site in the 5' non-coding region and downstream the lysosomal targeting sequence of the CathD cDNA, but not the catalytic region [41]. This HindIII fragment was then inserted, in appropriately prepared pcDNA3 vector, in front of the HA1-tagged Asp119Ala aequorin (Aeq) mutant [42] obtaining the CathD-Aeq chimera. Both probes were transfected into HeLa cells using Lipofectamine 2000 reagent (Life Technologies, Milano, Italy) the day before the experiment. Transfected apo-aequorins were reconstituted in modified Krebs-Ringer buffer (KRB, 135 mM NaCl, 5 mM KCl, 0.4 mM KH_2PO_4, 1 mM $MgSO_4$, 5.5 mM glucose, 20 mM HEPES (pH 7.4) supplemented with 600 μM EGTA , 5μM coelenterazine n and 300 μM ionomycin (all reagents from Sigma) for 1 h at 4°C. After reconstitution the cells were washed 3 times with KRB containing 600 μM EGTA and 2% BSA, followed by 3 washes with KRB containing 100 μM EGTA after which the coverslips were transferred into perfusion chamber of a custom built aequorinometer (CAIRN research, UK). The cells were perfused with KRB containing 100 μM EGTA at 37°C. After 3 min of baseline recording the perfusion solution was switched to KRB supplemented with 2 mM Ca^{2+} and recording continued until the $[Ca^{2+}]$ in the EL or ER did reach the steady-state level. At the end of each experiment, for quantification of the intra-organellar Ca^{2+} levels, the cells were perfused with distilled water containing 100 mM Ca^{2+} and 100 μM digitonin to discharge the remaining Aeq pool. The light signals were calibrated off-line into $[Ca^{2+}]$ values using an algorithm developed by Brini and coworkers [43].

Fura-2 Ca^{2+} measurements

HeLa cells were loaded with 5 μM Fura-2 AM in presence of 0.02% of Pluronic-127 (both from Life Technologies) and 10 μM sulfinpyrazone in KRB containing 2 mM $CaCl_2$ (30 min, room temperature), after which the cells were washed and left for other 30 min to allow de-estherification of Fura-2. After that the coverslips were mounted into acquisition chamber and places on the stage of a Leica DMI6000 epifluorescent microscope equipped with S Fluor x40/1.3 objective. The probe was excited by alternate 340 and 380 nm using a Polychrome IV monochromator (Till Photonics, Munich, Germany) and the Fura-2 emission light was filtered through 520/20 bandpass filter and

collected by a cooled CCD camera (Hamamatsu, Japan). The fluorescence signals were acquired and processed using MetaFluor software (Molecular Device, Sunnyvale, CA, USA). To quantify the differences in the amplitudes of Ca^{2+} transients the ratio values were normalized using the formula $\Delta F/F_0$ (referred to as normalized Fura-2 ratio, "Norm. Fura ratio").

Immunocytochemistry

$1.5x10^4$ HeLa cells, grown on 13 mm coverslips in 24 w/plates, were transfected with 0.3 μg CD-Aeq cDNA using Lipofectamine 2000 reagent. After 24 h, cells were fixed with 4% formaldehyde, permeabilized with 0.1% Triton X-100 and probed with anti-hemagglutinin epitope (HA, Roche, Mannheim, Germany), anti-Lamp2b, anti-mannose-6-phosphate receptor (M6PR), anti- early endosome antigen 1 (EEA) (all from Abcam, Cambridge, UK) and anti-endoplasmic reticulum-Golgi intermediate compartment (ERGIC, Sigma) primary antibodies (all 1:50) in phosphate buffered saline (PBS) supplemented with 1% gelatine (1 h 37°C). The cells were then washed 3 times with PBS and secondary Alexa Fluor conjugated antibody (1:200) were applied in PBS with 1% gelatine for 1 h at RT. The coverslips were then washed and mounted on a glass slides using FluoroShield mounting medium (Sigma). The cells were examined using a Leica DMI6000 epifluorescent microscope equipped with S Fluor x40/1.3 objective. Fluorescent signals were acquired and processed using Leica-Metamorph software.

Chemicals

All chemicals were of analytical grade and obtained from Sigma.

Results

NAADP induces Ca^{2+}-dependent non-selective cationic currents mediated by TRPM4 in HeLa cells

The whole-cell patch-clamp configuration was utilized to dyalise the cells with an intracellular solution containing 10 nM NAADP and record the subsequent bioelectrical response. This manoeuvre permits to detect NAADP-induced changes in sub-membranal Ca^{2+} concentration, as shown in earlier studies conducted in mammalian cells [35, 36, 44, 45]. Currents were measured by applying consecutive 400-ms voltage spanning -90 mV to +90 mV starting from a holding potential of 0 mV. The cytosolic infusion of NAADP induced tonic inward (at -80 mV) and outward (at +80 mV) currents with an average latency of 182.9 ± 21.2 sec (n = 51) in 51 out of 68 cells (Fig. 1A). These currents could either be sustained over time (as shown in Fig. 1A and Fig. 1E) or rapidly decay to the baseline (as shown in Fig. 1G). In the remaining 17 cells, the inclusion of NAADP in the patch-pipette elicited membrane current oscillations at both -80 mV and +80 mV after an average delay of 119.7 ± 31.7 sec (n = 17) (Fig. 1C). There was no significant difference in the lag time of the bioelectrical response to NAADP between tonic and spiking cells ($p < 0.05$). The I-V relationship of NAADP-evoked ionic currents was measured by subtracting the background I-V curve to that obtained after full development of the current (Fig. 1B) or at the oscillation peak (Fig. 1D), depending on the pattern of the signal. In both cases, it did not show any detectable rectification and reversed at around 0 mV: as expected, the reversal potential (E_{rev}) of NAADP-induced currents measured in tonic cells (4.5 ± 1.1 mV, n = 41) was not significantly different ($p<0.05$) from that obtained in oscillating ones (6.3 ± 1.9 mV, n = 14). Therefore, the biophysical characterization of NAADP-induced currents reveals that the same conductance is activated in both non-spiking and spiking cells, and the data collected from both cell types were computed together in subsequent experiments. The hallmarks of NAADP receptors in mammalian cells are their homologous desensitization at high NAADP doses and their sensitivity to Ned-19, which blocks the binding site for NAADP [9]. Consistent with these features, the amplitude of NAADP-induced currents in HeLa cells was significantly reduced by either of the following treatments: 1) cytosolic dialysis of 50-100 μM NAADP (Fig. 1E and Fig. 1F) or 2) inclusion of Ned-19 (10 μM) in the patch-pipette (Fig. 1G and Fig. 1H).

The fact that NAADP-induced currents invert polarity at potentials close to 0 mV suggests they are carried by a non-selective cation channel [36, 37, 44]. In agreement with this hypothesis, the replacement of extracellular Na^+ with an equimolar amount of the non-permeable $NMDG^+$ suppressed the inward current, while only slightly affecting the outward component, and caused a

shift of E_{rev} towards more negative values (Fig. 2A and Fig. 2B). In the same cells, removal of extracellular Ca^{2+} (0 Ca^{2+}) did not exert any effect both on the amplitude and on the polarity of NAADP-induced currents (Fig. 2A). Conversely, when K^+ in the intracellular solution was substituted with NMDG, the outward current was abrogated and the I-V relationship did not reverse even at +90 mV (Fig. 2C and Fig. 2D). Overall, these results indicate that NAADP activates a non-selective cation channel that conducts both Na^+ and K^+, but not Ca^{2+}. Melastatin transient receptor potential channel 4 (TRPM4) is a well known Ca^{2+}-activated non-selective cation conductance that is impermeable to Ca^{2+} [46]. In order to assess whether this is the membrane pathway recruited by NAADP in HeLa cells, we probed the effect of several TRPM4 blockers. Trivalent cations are widely employed to inhibit TRP channels at high micromolar concentrations [47, 48], while flufenamic acid (FFA) and 9-phenanthrol (9-Phen) are selective inhibitors of TRPM4 [46]. As depicted in Figure 2E and Figure 2F, 30 min pre-treatment with either La^{3+} (50 μM), Gd^{3+} (50 μM), FFA (20 μM) or 9-Phen (30 μM) abolished NAADP-elicited currents in HeLa cells. This pharmacological profile is compatible with TRPM4 engagement by intracellularly infused NAADP. In agreement with this hypothesis, NAADP did not activate any current when 10 mM EGTA was included in the recording pipette to prevent any increase in $[Ca^{2+}]_i$ (Fig. 2G). Preliminary experiments showed that the cytosolic dialysis of 10 mM EGTA does not trigger any current in the absence of NAADP, which indicates that store-operated Ca^{2+} entry (SOCE) is not activated under these conditions (n = 8; data not shown). Taken together, these results demonstrate that NAADP stimulates TRPM4 by causing a cytosolic elevation in $[Ca^{2+}]_i$ upon the mobilization of an intracellular Ca^{2+} pool, as indirectly confirmed by the lack of effect of 0 Ca^{2+} saline (Fig. 2A). TRPM4-mediated currents may, therefore, be utilized to monitor the intracellular Ca^{2+} response to NAADP in HeLa cells, as shown in other cell types [36, 45].

Acidic store blockers impair NAADP-induced Ca^{2+} signals in HeLa cells

A number of drugs are currently exploited to disrupt Ca^{2+} storage by acidic organelles and prevent NAADP-induced intracellular Ca^{2+} release [7, 9, 24]. GPN promotes osmotic bursting of lysosomes, bafilomycin A1 prevents EL vesicle acidification and their consequent intralumenal Ca^{2+} sequestration, and nigericin dissipates the proton gradient [32]. Each protocol described in the following experiments has been widely utilized to interfere with EL function and affect NAADP-evoked Ca^{2+} discharge [7, 9]. Pre-incubating the cells with GPN (200 μM, 1 hour) (Fig. 3A-3BB) and bafilomycin A1 (100 nM, 1 hour) (Fig. 3C-3D), significantly ($p<0.05$) reduced NAADP-elicited currents, while nigericin (50 μM, 20 min) fully suppressed them (Fig. 3E-3F). This result

indicates that Ca^{2+}-mobilization from acidic organelles contributes to TRPM4 activation by NAADP HeLa cells.

Thapsigargin-sensitive Ca^{2+} pools contribute to shape NAADP-elicited increase in $[Ca^{2+}]_i$

The contribution of $InsP_3$- and ryanodine-sensitive Ca^{2+} stores to NAADP signalling in HeLa cells was then probed by first pre-treating the cells with thapsigargin (2 μM, 1 hour) to deplete Ca^{2+} from ER [49]. This treatment abolished the Ca^{2+} response to NAADP in HeLa cells (Fig. 4A and Fig. 4D). Likewise, direct delivery of heparin (1 mg/ml) along with NAADP through the patch pipette to block $InsP_3$Rs [3] significantly ($p<0.05$) decreased both the amplitude and the duration of NAADP-induced Ca^{2+} release (Fig. 4B and Fig. 4D). Finally, the pharmacological inhibition of RyRs with either ryanodine or tetracaine abrogated the onset of NAADP-evoked Ca^{2+} signals [50]. In mode detail, intracellular dialysis from a patch pipette of ryanodine (100 μM) along with NAADP suppressed the ensuing Ca^{2+} mobilization in 2 out of 6 cells (Fig. 4C) and significantly ($p < 0.05$) reduced the magnitude of the Ca^{2+} transient occurring in the remaining 4 (Fig. 4D). Similarly, cytosolic infusion of tetracaine (100 μM) prevented the development of the Ca^{2+} response to NAADP (Fig. 4C and Fig. 4D). Collectively, these results suggest that RyRs directly participate to the generation of NAADP-evoked Ca^{2+} signals, while $InsP_3$R are required to sustain them over time. It turns out that both EL and ER Ca^{2+} stores shape the Ca^{2+} response to NAADP in HeLa cells.

GPN, bafilomycin 1 and nigericin inhibit Ca^{2+} sequestration by both endo-lysosomes and endoplasmic reticulum

Once established that both acidic organelles and the ER are recruited by NAADP to induce intracellular Ca^{2+} signals in HeLa cells, we harnessed aequorin-based Ca^{2+} fluorophores to assess the effects of GPN, bafilomycin A1, nigericin, and thapsigargin on both ER and EL Ca^{2+} filling. To assess the extent of Ca^{2+} filling of lysosomal lumen, we have generated a new lysosome-targeted Aeq probe by fusing full-length cathepsin D cDNA to the N-terminus of HA1-Aeq(mut) cassette under control of CMV promoter, designated as CathD-Aeq (Supplementary Fig. 1A). Immunocytochemical analysis of CathD-AEQ, expressed in HeLa cells, revealed co-localisation of the probe with the lysosomal marker Lamp2b (Supplementary Fig. 1B-a) and with the late endosomal marker M6PR (Supplementary Fig. 1B-b), but not with markers of early endosomes (EEA; Supplementary Fig. 1B-c) or with the ER marker (Ergic; Supplementary Fig. 1B-d), thus indicating correct sorting of CathD-Aeq probe to EL compartments [51]. Both ER and EL Aeq probes bear a single amino acid (Asp119→Ala) substitution to decrease the affinity of Aeq to Ca^{2+}

[52]. First, we assured that Aeq(mut) functions properly at the acidic pH (4.5-5.5) of the endo-lysosomal lumen and the results may be compared with those of the ER-Aeq. We quantified the light emitted by Aeq(mut) in lysates prepared from transfected HeLa cells with pH ranging form 3.85 to 7.5 upon addition of 100 mM Ca^{2+}, and we found that at the extreme acidic pH 3.85 there was nonsignificant increase of the emitted light by about 10% as compared with that emitted at pH 7 (Supplementary Fig. 1C), demonstrating that Aeq(mut) is functional in acidic conditions and may be used for Ca^{2+} measurements in EL organelles. Next, we checked whether CathD-Aeq correctly reports Ca^{2+} concentrations in acidic conditions. Supplementary Fig. 1D shows that addition 50 μM Ca^{2+} results in robust detection of [Ca^{2+}] in the entire pH range from pH 3.85 to pH 7. Next, we compared the steady state Ca^{2+} levels in ER and EL lumens. Direct measurement of the EL Ca^{2+} content revealed that rate of refilling and steady state level of Ca^{2+} in the EL compartment were not different from those of the ER (Fig. 5A and B), thereby confirming previous indirect estimations of high EL Ca^{2+} content [53, 54].

Next, we investigated whether pharmacological disruption of acidic stores specifically affects EL Ca^{2+} dynamics. Unexpectedly, GPN exerted a dose-dependent inhibition of Ca^{2+} uptake not only by EL organelles (Fig. 5A), but also by the ER Ca^{2+} pool (Fig. 5B). In particular, at 200 μM (20 min pre-treatment), the effect of GPN was even more pronounced for ER loading (36.3 ± 15.9 % *vs.* control samples, p = 0.009) (Fig. 5B), as compared to EL Ca^{2+} uptake (65.3 ± 15.4 % *vs.* control samples, p = 0.012) (Fig. 5A). Similarly, overnight pre-incubation with 100 nM bafilomycin A1 hindered Ca^{2+} sequestration by both EL (Fig. 6A) and ER (Fig. 6B) compartments, although the inhibition of EL Ca^{2+} loading was slightly larger (49.2 ± 4.5 % *vs.* control, p = 1.7e-6) than ER Ca^{2+} refilling (65.9 ± 9.03 % *vs.* control, p = 2.5e-5) (Fig. 6). Likewise, nigericin (50 μM, 20 min) dose-dependently decreased Ca^{2+} uptake in both EL and ER compartments (Fig. 7). 20 μM nigericin inhibited to the same extent both EL (31.8 ± 12 % *vs.* control, p = 0.00036) and ER (33.3 ± 9.9 % *vs.* control, p = 8.2e-5) Ca^{2+} uptake (Fig. 7). Overall, these results clearly indicate that the pharmacological disruption of lysosomal Ca^{2+} content leads to a dramatic reduction in ER Ca^{2+} levels as well.

Inhibitors of SERCA pump block Ca^{2+} sequestration by both endoplasmic reticulum and endo-lysosomes

Next, we investigated whether specific SERCA blockers, such as thapsigargin and tBHQ, impact on EL Ca^{2+} sequestration. Fig. 8 shows that thapsigargin (20 nM, 10 min) prevented Ca^{2+} uptake into both EL (Fig. 8A) and ER (Fig. 8B) compartments. However, 5 nM thapsigargin was ineffective on EL (Fig. 8A), but not ER Ca^{2+} sequestration (69.8 ± 17.7% *vs.* control, p = 4e-6) (Fig.

8B). In the same way, 100 μM tBHQ, a SERCA antagonist that binds to a different site with respect to thapsigargin, suppressed Ca^{2+} uptake in both endo-lysosomes and ER (Fig. 8). A recent study suggested that tBHQ and high concentrations of thapsigargin may also target lysosomal SERCA3 [55], but this finding is likely to be confined to human platelets [24]. In addition, EL Ca^{2+} uptake is abrogated by low nM doses of thapsigargin, which is ineffective on this SERCA isoform [55]. Therefore, it is conceivable that both thapsigargin and tBHQ inhibit SERCA-mediated Ca^{2+} sequestration into ER under our conditions. It turns out that EL Ca^{2+} refilling depends on the proper Ca^{2+} uptake by ER in HeLa cells.

GPN, bafilomycin A1, and nigericin affect intracellular Ca^{2+} release by tBHQ

The results hitherto obtained provided the evidence that lysosomotropic agents, such as GPN, bafilomycin A1, and nigericin, interfere with ER Ca^{2+} filling. On the other hand, well established inhibitors of SERCA activity prevent EL Ca^{2+} sequestration as well. To consolidate these findings and further analyze the interaction between EL and ER Ca^{2+} stores, we took advantage from single cell imaging of fura-2/AM-loaded cells to assess whether the pharmacological blockade of EL Ca^{2+} uptake affects ER Ca^{2+} levels. As expected [27, 56], the induction of osmotic bursting with GPN (200 μM) in the absence of extracellular Ca^{2+} (0 Ca^{2+}) elicited a Ca^{2+} transient which lasted for about 5 min (Fig. 9A, grey tracing). Perfusion of vehicle (DMSO) to control cells did not change cytosolic Ca^{2+} levels (Fig. 9A, black tracing). After GPN-induced $[Ca^{2+}]_i$ rise, tBHQ (20 μM) was added to the perfusion medium to examine ER Ca^{2+} content. In control experiments, tBHQ produced an elevation in $[Ca^{2+}]_i$ due to passive emptying of the ER Ca^{2+} pool (black tracing and column in Figure 9A). However, GPN pre-treatment significantly reduced the amplitude of the following Ca^{2+} response to tBHQ (12.8 ± 4.4 % *vs.* control, p = 2e-19) (grey tracing and column in Fig. 9A). In an inverted experimental setting, when the ER Ca^{2+} stores were first emptied by tBHQ (20 μM, 10 min) and $[Ca^{2+}]_i$ returned to the near-baseline level, application of GPN (200 μM) essentially failed to elevate Ca^{2+} in the cytosol (33.17 ± 22.56 % *vs.* control, p = 2e-37) (Fig. 9B). Unlike GPN, acute addition of bafilomycin A1 (1 μM) did not alter resting Ca^{2+} levels in HeLa cells (not shown), while over-night pre-incubation with 100 nM bafilomycin A1 significantly reduced the magnitude of tBHQ-induced intracellular Ca^{2+} mobilization (53.3 ± 22.3 % *vs.* control, p = 4e-34) (Fig. 9C). Finally, nigericin (50 μM) evoked a biphasic increase in $[Ca^{2+}]_i$ which returned to the baseline within 5 minutes and dampened the subsequent tBHQ-induced Ca^{2+} signal (36.8 ± 23 % *vs.* control, p = 5e-18) (Fig. 9D). Overall, these data confirm that the disruption of the EL Ca^{2+} pool interferes with ER Ca^{2+} loading and *viceversa*. As a consequence of the functional cross-talk between these two Ca^{2+} storage compartments,

extreme caution is warranted when drawing any conclusion on the intracellular target(s) recruited by NAADP exclusively on the basis of pharmacological manipulation.

Discussion

NAADP is the most suitable intracellular messenger to either discharge intraluminally stored Ca^{2+} [7, 9, 16] or to gate Ca^{2+} inflow in response to extracellular stimulation [2, 12, 14, 57], thereby regulating a host of cellular functions. While TPCs have been clearly established to mobilize Ca^{2+} from acidic lysosome-like vesicles in sea urchin eggs [58], the target organelle(s) and cognate receptor(s) of NAADP in mammalian cells are far from being clearly elucidated [7, 9, 18-20]. The controversial issue as to whether NAADP serves as a triggering signal to initiate intracellular Ca^{2+} waves by recruiting either $InsP_3Rs$ and/or RyRs upon lysosomal Ca^{2+} release or it directly activates ER-located RyRs has been fuelled by our poor knowledge of the ER-EL Ca^{2+} cross-talk [28, 59, 60]. This deficit in our knowledge of the basic mechanisms of organellar interaction might have biased the interpretation of many data produced by the pharmacological manipulation of the multiple Ca^{2+} pools endowed to mammalian cells [61]. Accordingly, convincing evidence has been provided to demonstrate that, apart from the anterograde Ca^{2+} signal delivered from the acidic stores to ER, ER itself can signal in a retrograde fashion to acidic vesicles [27-31]. This bidirectional Ca^{2+} chatter controls intraluminal Ca^{2+} levels in both compartments, a feature that should be taken into account both when disrupting EL Ca^{2+} accumulation and when depleting ER Ca^{2+} stores. Therefore, we accomplished the present investigation to understand: 1) whether and how classic inhibitors of ER- and EL-dependent Ca^{2+} release affect NAADP-induced Ca^{2+} signals in HeLa cells; 2) whether interfering with ER Ca^{2+} sequestration impairs EL Ca^{2+} uptake and *viceversa*; and 3) to assess the functional implications of this Ca^{2+}-mediated cross-talk for NAADP-evoked Ca^{2+} signals.

The “whole-cell” patch-clamp technique has been widely employed to investigate the Ca^{2+} response to NAADP by monitoring the activation of Ca^{2+}-dependent non-selective cation channels [35, 36, 44, 45]. This sophisticated tool enables to detect sub-membranal Ca^{2+} elevations that may be missed by utilizing epifluorescence or confocal Ca^{2+} imaging [37]. The following pieces of evidence suggest that the ion currents recorded in HeLa cells dyalized with NAADP truly reflect a concomitant increase in cytosolic Ca^{2+} concentration. First, NAADP triggers either single, long lasting or oscillatory membrane currents which disappear if NAADP is omitted from the patch pipette or if EGTA is supplemented to the intracellular solution to buffer cytosolic Ca^{2+}. EGTA is a slow Ca^{2+} buffer which is normally effective at preventing global changes in $[Ca^{2+}]_i$ [44, 62]. Therefore, we speculate that the Ca^{2+} response to NAADP takes place in the bulk cytosol rather than being confined to the sub-membranal domain. Second, the magnitude of NAADP-induced Ca^{2+}

currents is significantly reduced when NAADP is infused at 50-100 μM, which is fully consistent with the well known desensitization of mammalian NAADP receptors in the high micromolar range [9]. Third, the Ca^{2+} response to NAADP is abrogated by Ned-19, which selectively antagonizes NAADP binding to its receptor site [9, 63]. Thus, NAADP triggers the activation of Ca^{2+}-dependent currents in HeLa cells, thereby rendering these cells a suitable model to investigate the underlying Ca^{2+} stores. The Ca^{2+}-sensitive membrane conductance recruited by NAADP under our conditions is likely to be mediated by TRPM4. First, NAADP-induced currents display the same biophysical features, i.e. linear I-V relationship, E_{rev} close to 0 mV, permeability to the monovalent cations Na^+ and Cs^+, but not to Ca^{2+}, as TRPM4-mediated currents both in naïve cells [64-66] and in heterologous expression systems [67]. Second, the pharmacological profile of NAADP-elicited currents is fully compatible with that of TRPM4 [46, 47]. Third, a functional TRPM4 protein is expressed in HeLa cells, albeit its endogenous biophysical and pharmacological properties are yet to be evaluated [68]. In this view, NAADP has long been known to activate Ca^{2+}-dependent non-selective cation currents in mouse pancreatic β-cells [36, 45], which are abrogated following pharmacological inhibition of TRPM4 [32]. Conversely, NAADP-evoked membrane depolarization in neurons of the rat medulla oblongata has been ascribed to TRPM2 stimulation, as the underlying current is conducted by extracellular Ca^{2+} and requires intracellular Ca^{2+} release to develop [44].

The pharmacological manipulation of the intracellular Ca^{2+} pools carried out by utilizing a number of drugs affecting either ER (i.e. thapsigargin, CPA and tBHQ) or endolysosomal (i.e. GPN, bafilomycin A1, and nigericin) Ca^{2+} content led to the proposal of the trigger hypothesis, according to which NAADP induces a local Ca^{2+} discharge from acidic stores thereby eliciting a secondary larger discharge from the ER [7, 9]. Alternatively, NAADP may directly stimulate RyRs to give raise to a regenerative Ca^{2+} wave which is independent on the activation of the EL Ca^{2+} store [19, 20]. In order to dissect the signalling pathways downstream NAADP infusion in HeLa cells, we sought to selectively abrogate either ER- or EL-dependent Ca^{2+} mobilization. We found that the disruption of the acidic Ca^{2+} reservoir with three different drugs (i.e. GPN by inducing osmotic lysis of organelles containing the lysosomal hydrolase cathepsin C; bafilomycin A1 preventing vesicle acidification; nigericin by dissipating the proton gradient across the organelle membrane, , thereby preventing pH-dependent accumulation of Ca^{2+} in the acidic compartment) hindered NAADP-induced currents. Similarly, the bioelectrical response to NAADP was abated by previous depletion of the ER Ca^{2+} pool with thapsigargin and by RyR inhibition with ryanodine and tetracaine. The blockade of $InsP_3Rs$ with heparin did not suppress the current, but it significantly reduced both its amplitude and duration. Taken together, these results suggest that both ER and EL

Ca^{2+} stores are recruited to shape the Ca^{2+} response to NAADP in HeLa cells. One could argue that the Ca^{2+} trigger model would nicely fit these results, thereby suggesting that NAADP stimulates TPCs to release Ca^{2+} from acidic stores and engage the neighbouring RyRs and $InsP_3Rs$ through the mechanism of CICR. Consistently, over-expression of TPC2 has been shown to enhance NAADP-elicited Ca^{2+} signalling in HeLa cells [69]. A recent series of elegant studies conducted by three separate groups have, however, unveiled the bidirectional nature of Ca^{2+} movements occurring at the ER-EL interface [29, 31, 60]. In addition of being directly loaded into ER lumen following NAADP-dependent TPC activation [4, 16, 17], Ca^{2+} can be sequestered back into EL Ca^{2+} stores upon ER-induced Ca^{2+} mobilization [29, 31, 60]. This Ca^{2+}-mediated cross-talk between two physically distinct Ca^{2+} pools might bias any conclusion drawn based on the selective inhibition of Ca^{2+} uptake by each of them. Therefore, we exploited optical reporters specifically generated to monitor Ca^{2+} uptake into EL and ER lumen, respectively, to assess whether the pharmacological manipulation of the ER Ca^{2+} pool interferes with ER Ca^{2+} storage and *viceversa*. As expected, GPN, bafilomycin A1 and nigericin inhibited Ca^{2+} accumulation within EL vesicles, as well as thapsigargin and tBHQ prevented SERCA-mediated Ca^{2+} sequestration into the ER. Nevertheless, disrupting EL ability to store Ca^{2+} significantly reduced ER Ca^{2+} content and, *viceversa*, the inhibition of SERCA activity prevented Ca^{2+} loading into acidic organelles. These results might be explained by the reciprocal sensing and control of Ca^{2+} levels in one store by another. According to the protocol applied in experiments described in Figures 5-8, at point zero all intracellular Ca^{2+} stores are nominally depleted by the incubation in presence of EGTA and ionomycin. When Ca^{2+} is re-added to the cells, it is assumed to simultaneously reach the Ca^{2+} transporters of both EL and ER membranes. If the Ca^{2+} content of two organelles were independently regulated, the inhibition of Ca^{2+} uptake by one store would not affect the uptake by the other one. It appears, however, that the transport of Ca^{2+} into EL compartment is blocked when Ca^{2+} uptake into ER is inhibited and *viceversa*. In other words, to have functional Ca^{2+} uptake by either EL or ER, its counterpart must have a certain level of Ca^{2+} in its lumen or the Ca^{2+} transporting system active. Thus, it might be speculated that in HeLa cells, EL and ER reciprocally sense and control the Ca^{2+} filling of the adjacent organelle. This might be realised through an agonist-induced Ca^{2+} elevation but might also be via Ca^{2+} leakage mechanism, perhaps through constitutively open TPCs, RyRs or $InsP_3Rs$. These data suggests that Ca^{2+} accumulation within both compartments requires a tight and finely tuned Ca^{2+} exchange at the ER-EL interface and builds a new level of complexity to our understanding of control of cellular Ca^{2+} homeostasis [60]. Consequently, the blockade of Ca^{2+} refilling into either of the two Ca^{2+} pools leads to an appreciable decrease in the intraluminal Ca^{2+} levels of the other. Consistently, Fura-2 imaging experiments revealed that: 1) pre-treating HeLa cells with GPN,

bafilomycin A1, and nigericin abrogated the subsequent Ca^{2+} response to tBHQ, which supports the notion that the ER Ca^{2+} reservoir is depleted by emptying the EL Ca^{2+} pool; and 2) pre-incubating the cells with tBHQ prevented the elevation in $[Ca^{2+}]_i$ induced by directly liberating EL Ca^{2+}. These findings support the aequorin experiment on bi-directional control of Ca^{2+} load, and are corroborated by the observations that all the studies addressing ER-EL interactions reported a close (about 20 nm) apposition between acidic organelles and ER tubules [27-29, 31]. It turns out that establishing the sub-cellular location of the first Ca^{2+} deposit activated by NAADP exclusively based on the sensitivity of NAADP-evoked Ca^{2+} signals to SERCA blockers, GPN, bafilomycin A1 and nigericin may lead to unreliable conclusions. The observation that TPC2 is indispensable for triggering NAADP-induced Ca^{2+} signals in HeLa cells concurs in favour of EL involvement in the onset of their Ca^{2+} response [69]. However, our data strongly suggest that the effect of lysosome manipulation on ER Ca^{2+} handling and *viceversa* should be carefully evaluated to prevent any misleading interpretation of data engendered by the selective disruption of intracellular Ca^{2+} stores, as recently illustrated in mouse hippocampal neurons and astrocytes [34], HEK293 cells [29], human skin fibroblasts [27], and mouse primary pancreatic β-cells [32, 33].

In conclusion, the present manuscript provides the evidence that a functional coupling does exist at the ER-EL interface and maintains the proper Ca^{2+} levels within both compartments. This feature might be relevant to the regulation of Ca^{2+}-dependent EL functions, such as control of lysosomal pH and enzyme activity, vesicle trafficking and TPC gating [28, 31, 60], under both physiological and pathological (i.e. Niemann-Pick type C disease, amyotrophic lateral sclerosis and Alzheimer's disease) conditions. Likewise, it will be intriguing to investigate whether any imbalance in steady state ER Ca^{2+} concentration, that may dictate either pro-survival or pro-apoptotic programs depending on how intraluminal Ca^{2+} levels vary [70], is underpinned by parallel changes in ER Ca^{2+} content. As a consequence, extreme caution is warranted when drawing straightforward conclusions about the sub-cellular location of NAADP-sensitive stores by exclusively relying on pharmacological tools.

References

[1] A. Galione, A.J. Morgan, A. Arredouani, L.C. Davis, K. Rietdorf, M. Ruas, J. Parrington, NAADP as an intracellular messenger regulating lysosomal calcium-release channels, Biochem Soc Trans, 38 (2010) 1424-1431.
[2] D. Lim, K. Kyozuka, G. Gragnaniello, E. Carafoli, L. Santella, NAADP+ initiates the Ca2+ response during fertilization of starfish oocytes, FASEB J, 15 (2001) 2257-2267.
[3] F. Moccia, G.A. Nusco, D. Lim, K. Kyozuka, L. Santella, NAADP and InsP3 play distinct roles at fertilization in starfish oocytes, Dev Biol, 294 (2006) 24-38.
[4] T.P. Collins, R. Bayliss, G.C. Churchill, A. Galione, D.A. Terrar, NAADP influences excitation-contraction coupling by releasing calcium from lysosomes in atrial myocytes, Cell Calcium, 50 (2011) 449-458.
[5] G.C. Brailoiu, B. Gurzu, X. Gao, R. Parkesh, P.K. Aley, D.I. Trifa, A. Galione, N.J. Dun, M. Madesh, S. Patel, G.C. Churchill, E. Brailoiu, Acidic NAADP-sensitive calcium stores in the endothelium: agonist-specific recruitment and role in regulating blood pressure, J Biol Chem, 285 (2010) 37133-37137.
[6] R. Masgrau, G.C. Churchill, A.J. Morgan, S.J. Ashcroft, A. Galione, NAADP: a new second messenger for glucose-induced Ca2+ responses in clonal pancreatic beta cells, Curr Biol, 13 (2003) 247-251.
[7] A. Galione, J. Parrington, T. Funnell, Physiological roles of NAADP-mediated Ca2+ signaling, Sci China Life Sci, 54 (2011) 725-732.
[8] F. Moccia, R. Berra-Romani, F. Tanzi, Update on vascular endothelial Ca2+ signalling: A tale of ion channels, pumps and transporters, World J Biol Chem, 3 (2012) 127-158.
[9] A. Galione, NAADP receptors, Cold Spring Harb Perspect Biol, 3 (2011) a004036.
[10] A. Galione, G.C. Churchill, Interactions between calcium release pathways: multiple messengers and multiple stores, Cell Calcium, 32 (2002) 343-354.
[11] G.C. Churchill, J.S. O'Neill, R. Masgrau, S. Patel, J.M. Thomas, A.A. Genazzani, A. Galione, Sperm deliver a new second messenger: NAADP, Curr Biol, 13 (2003) 125-128.
[12] A.J. Morgan, Sea urchin eggs in the acid reign, Cell Calcium, 50 (2011) 147-156.
[13] F. Moccia, R.A. Billington, L. Santella, Pharmacological characterization of NAADP-induced Ca2+ signals in starfish oocytes, Biochem Biophys Res Commun, 348 (2006) 329-336.
[14] F. Moccia, D. Lim, G.A. Nusco, E. Ercolano, L. Santella, NAADP activates a Ca2+ current that is dependent on F-actin cytoskeleton, FASEB J, 17 (2003) 1907-1909.
[15] F. Moccia, D. Lim, K. Kyozuka, L. Santella, NAADP triggers the fertilization potential in starfish oocytes, Cell Calcium, 36 (2004) 515-524.
[16] G.C. Churchill, A. Galione, NAADP induces Ca2+ oscillations via a two-pool mechanism by priming IP3- and cADPR-sensitive Ca2+ stores, EMBO J, 20 (2001) 2666-2671.
[17] A. Macgregor, M. Yamasaki, S. Rakovic, L. Sanders, R. Parkesh, G.C. Churchill, A. Galione, D.A. Terrar, NAADP controls cross-talk between distinct Ca2+ stores in the heart, J Biol Chem, 282 (2007) 15302-15311.
[18] A.H. Guse, Linking NAADP to ion channel activity: a unifying hypothesis, Sci Signal, 5 (2012) pe18.
[19] W. Dammermann, B. Zhang, M. Nebel, C. Cordiglieri, F. Odoardi, T. Kirchberger, N. Kawakami, J. Dowden, F. Schmid, K. Dornmair, M. Hohenegger, A. Flügel, A.H. Guse, B.V. Potter, NAADP-mediated Ca2+ signaling via type 1 ryanodine receptor in T cells revealed by a synthetic NAADP antagonist, Proc Natl Acad Sci U S A, 106 (2009) 10678-10683.
[20] M. Hohenegger, J. Suko, R. Gscheidlinger, H. Drobny, A. Zidar, Nicotinic acid-adenine dinucleotide phosphate activates the skeletal muscle ryanodine receptor, Biochem J, 367 (2002) 423-431.
[21] A. Jha, E. Brailoiu, S. Muallem, How does NAADP release lysosomal Ca (2+)?, Channels (Austin), 8 (2014) 174-175.

[22] A.J. Morgan, A. Galione, Two-pore channels (TPCs): current controversies, Bioessays, 36 (2014) 173-183.
[23] J.S. Marchant, S. Patel, Questioning regulation of two-pore channels by NAADP, Messenger (Los Angel), 2 (2013) 113-119.
[24] A.J. Morgan, F.M. Platt, E. Lloyd-Evans, A. Galione, Molecular mechanisms of endolysosomal Ca2+ signalling in health and disease, Biochem J, 439 (2011) 349-374.
[25] S. Patel, R. Docampo, Acidic calcium stores open for business: expanding the potential for intracellular Ca2+ signaling, Trends Cell Biol, 20 (2010) 277-286.
[26] B. Esposito, G. Gambara, A.M. Lewis, F. Palombi, A. D'Alessio, L.X. Taylor, A.A. Genazzani, E. Ziparo, A. Galione, G.C. Churchill, A. Filippini, NAADP links histamine H1 receptors to secretion of von Willebrand factor in human endothelial cells, Blood, 117 (2011) 4968-4977.
[27] B.S. Kilpatrick, E.R. Eden, A.H. Schapira, C.E. Futter, S. Patel, Direct mobilisation of lysosomal Ca2+ triggers complex Ca2+ signals, J Cell Sci, 126 (2013) 60-66.
[28] A.K. Lam, A. Galione, The endoplasmic reticulum and junctional membrane communication during calcium signaling, Biochim Biophys Acta, 1833 (2013) 2542-2559.
[29] C.I. López-Sanjurjo, S.C. Tovey, D.L. Prole, C.W. Taylor, Lysosomes shape Ins(1,4,5)P3-evoked Ca2+ signals by selectively sequestering Ca2+ released from the endoplasmic reticulum, J Cell Sci, 126 (2013) 289-300.
[30] L. McGuinness, S.J. Bardo, N.J. Emptage, The lysosome or lysosome-related organelle may serve as a Ca2+ store in the boutons of hippocampal pyramidal cells, Neuropharmacology, 52 (2007) 126-135.
[31] A.J. Morgan, L.C. Davis, S.K. Wagner, A.M. Lewis, J. Parrington, G.C. Churchill, A. Galione, Bidirectional Ca^{2+} signaling occurs between the endoplasmic reticulum and acidic organelles, J Cell Biol, 200 (2013) 789-805.
[32] A. Arredouani, A.M. Evans, J. Ma, J. Parrington, M.X. Zhu, A. Galione, An emerging role for NAADP-mediated Ca2+ signaling in the pancreatic β-cell, Islets, 2 (2010) 323-330.
[33] J.G. Duman, L. Chen, A.E. Palmer, B. Hille, Contributions of intracellular compartments to calcium dynamics: implicating an acidic store, Traffic, 7 (2006) 859-872.
[34] V. Pandey, C.C. Chuang, A.M. Lewis, P.K. Aley, E. Brailoiu, N.J. Dun, G.C. Churchill, S. Patel, Recruitment of NAADP-sensitive acidic Ca2+ stores by glutamate, Biochem J, 422 (2009) 503-512.
[35] P.J. Calcraft, M. Ruas, Z. Pan, X. Cheng, A. Arredouani, X. Hao, J. Tang, K. Rietdorf, L. Teboul, K.T. Chuang, P. Lin, R. Xiao, C. Wang, Y. Zhu, Y. Lin, C.N. Wyatt, J. Parrington, J. Ma, A.M. Evans, A. Galione, M.X. Zhu, NAADP mobilizes calcium from acidic organelles through two-pore channels, Nature, 459 (2009) 596-600.
[36] J.M. Cancela, G.C. Churchill, A. Galione, Coordination of agonist-induced Ca2+-signalling patterns by NAADP in pancreatic acinar cells, Nature, 398 (1999) 74-76.
[37] F. Moccia, G.A. Nusco, D. Lim, E. Ercolano, G. Gragnaniello, E.R. Brown, L. Santella, Ca2+ signalling and membrane current activated by cADPr in starfish oocytes, Pflugers Arch, 446 (2003) 541-552.
[38] F. Moccia, C. Frost, R. Berra-Romani, F. Tanzi, D.J. Adams, Expression and function of neuronal nicotinic ACh receptors in rat microvascular endothelial cells, Am J Physiol Heart Circ Physiol, 286 (2004) H486-491.
[39] R. Takezawa, H. Cheng, A. Beck, J. Ishikawa, P. Launay, H. Kubota, J.P. Kinet, A. Fleig, T. Yamada, R. Penner, A pyrazole derivative potently inhibits lymphocyte Ca2+ influx and cytokine production by facilitating transient receptor potential melastatin 4 channel activity, Mol Pharmacol, 69 (2006) 1413-1420.
[40] C. Lazzari, C. Peggion, R. Stella, M.L. Massimino, D. Lim, A. Bertoli, M.C. Sorgato, Cellular prion protein is implicated in the regulation of local Ca2+ movements in cerebellar granule neurons, J Neurochem, 116 (2011) 881-890.

[41] P. Metcalf, M. Fusek, Two crystal structures for cathepsin D: the lysosomal targeting signal and active site, EMBO J, 12 (1993) 1293-1302.
[42] M. Bonora, C. Giorgi, A. Bononi, S. Marchi, S. Patergnani, A. Rimessi, R. Rizzuto, P. Pinton, Subcellular calcium measurements in mammalian cells using jellyfish photoprotein aequorin-based probes, Nat Protoc, 8 (2013) 2105-2118.
[43] M. Brini, R. Marsault, C. Bastianutto, J. Alvarez, T. Pozzan, R. Rizzuto, Transfected aequorin in the measurement of cytosolic Ca2+ concentration ([Ca2+]c). A critical evaluation, J Biol Chem, 270 (1995) 9896-9903.
[44] G.C. Brailoiu, E. Brailoiu, R. Parkesh, A. Galione, G.C. Churchill, S. Patel, N.J. Dun, NAADP-mediated channel 'chatter' in neurons of the rat medulla oblongata, Biochem J, 419 (2009) 91-97.
[45] J.M. Cancela, O.V. Gerasimenko, J.V. Gerasimenko, A.V. Tepikin, O.H. Petersen, Two different but converging messenger pathways to intracellular Ca(2+) release: the roles of nicotinic acid adenine dinucleotide phosphate, cyclic ADP-ribose and inositol trisphosphate, EMBO J, 19 (2000) 2549-2557.
[46] H. Abriel, N. Syam, V. Sottas, M.Y. Amarouch, J.S. Rougier, TRPM4 channels in the cardiovascular system: physiology, pathophysiology, and pharmacology, Biochem Pharmacol, 84 (2012) 873-881.
[47] L. Dwyer, P.L. Rhee, V. Lowe, H. Zheng, L. Peri, S. Ro, K.M. Sanders, S.D. Koh, Basally activated nonselective cation currents regulate the resting membrane potential in human and monkey colonic smooth muscle, Am J Physiol Gastrointest Liver Physiol, 301 (2011) G287-296.
[48] F. Moccia, S. Dragoni, F. Lodola, E. Bonetti, C. Bottino, G. Guerra, U. Laforenza, V. Rosti, F. Tanzi, Store-dependent Ca(2+) entry in endothelial progenitor cells as a perspective tool to enhance cell-based therapy and adverse tumour vascularization, Curr Med Chem, 19 (2012) 5802-5818.
[49] R. Berra-Romani, A. Raqeeb, J. Torres-Jácome, A. Guzman-Silva, G. Guerra, F. Tanzi, F. Moccia, The mechanism of injury-induced intracellular calcium concentration oscillations in the endothelium of excised rat aorta, J Vasc Res, 49 (2012) 65-76.
[50] D.J. West, A.J. Williams, Pharmacological regulators of intracellular calcium release channels, Current Pharmaceutical Design, 13 (2007) 2428-2442.
[51] J. Huotari, A. Helenius, Endosome maturation, EMBO J, 30 (2011) 3481-3500.
[52] M. Montero, M. Brini, R. Marsault, J. Alvarez, R. Sitia, T. Pozzan, R. Rizzuto, Monitoring dynamic changes in free Ca2+ concentration in the endoplasmic reticulum of intact cells, EMBO J, 14 (1995) 5467-5475.
[53] K.A. Christensen, J.T. Myers, J.A. Swanson, pH-dependent regulation of lysosomal calcium in macrophages, J Cell Sci, 115 (2002) 599-607.
[54] C.C. Scott, J. Gruenberg, Ion flux and the function of endosomes and lysosomes: pH is just the start: the flux of ions across endosomal membranes influences endosome function not only through regulation of the luminal pH, Bioessays, 33 (2011) 103-110.
[55] J.A. Rosado, Acidic Ca2+ stores in platelets, Cell Calcium, 50 (2011) 168-174.
[56] T. Haller, P. Dietl, P. Deetjen, H. Völkl, The lysosomal compartment as intracellular calcium store in MDCK cells: a possible involvement in InsP3-mediated Ca2+ release, Cell Calcium, 19 (1996) 157-165.
[57] I. Berg, B.V. Potter, G.W. Mayr, A.H. Guse, Nicotinic acid adenine dinucleotide phosphate ($NAADP^+$) is an essential regulator of T-lymphocyte Ca2+-signaling, J Cell Biol, 150 (2000) 581-588.
[58] G.C. Churchill, Y. Okada, J.M. Thomas, A.A. Genazzani, S. Patel, A. Galione, NAADP mobilizes Ca2+ from reserve granules, lysosome-related organelles, in sea urchin eggs, Cell, 111 (2002) 703-708.
[59] S. Patel, E. Brailoiu, Triggering of Ca2+ signals by NAADP-gated two-pore channels: a role for membrane contact sites?, Biochem Soc Trans, 40 (2012) 153-157.

[60] R. van der Kant, J. Neefjes, Small regulators, major consequences - Ca^{2+} and cholesterol at the endosome-ER interface, J Cell Sci, 127 (2014) 929-938.
[61] M.J. Berridge, M.D. Bootman, H.L. Roderick, Calcium signalling: Dynamics, homeostasis and remodelling, Nat Rev Mol Cell Biol, 4 (2003) 517-529.
[62] S. Patel, J.S. Marchant, E. Brailoiu, Two-pore channels: Regulation by NAADP and customized roles in triggering calcium signals, Cell Calcium, 47 (2010) 480-490.
[63] J.S. Marchant, Y. Lin-Moshier, T.F. Walseth, S. Patel, The Molecular Basis for Ca2+ Signalling by NAADP: Two-Pore Channels in a Complex?, Messenger (Los Angel), 1 (2012) 63-76.
[64] M.Y. Amarouch, N. Syam, H. Abriel, Biochemical, single-channel, whole-cell patch clamp, and pharmacological analyses of endogenous TRPM4 channels in HEK293 cells, Neurosci Lett, 541 (2013) 105-110.
[65] V. Marigo, K. Courville, W.H. Hsu, J.M. Feng, H. Cheng, TRPM4 impacts on Ca2+ signals during agonist-induced insulin secretion in pancreatic beta-cells, Mol Cell Endocrinol, 299 (2009) 194-203.
[66] H. Morita, A. Honda, R. Inoue, Y. Ito, K. Abe, M.T. Nelson, J.E. Brayden, Membrane stretch-induced activation of a TRPM4-like nonselective cation channel in cerebral artery myocytes, J Pharmacol Sci, 103 (2007) 417-426.
[67] N.D. Ullrich, T. Voets, J. Prenen, R. Vennekens, K. Talavera, G. Droogmans, B. Nilius, Comparison of functional properties of the Ca2+-activated cation channels TRPM4 and TRPM5 from mice, Cell Calcium, 37 (2005) 267-278.
[68] R. Armisén, K. Marcelain, F. Simon, J.C. Tapia, J. Toro, A.F. Quest, A. Stutzin, TRPM4 enhances cell proliferation through up-regulation of the β-catenin signaling pathway, J Cell Physiol, 226 (2011) 103-109.
[69] Y. Lu, B.X. Hao, R. Graeff, C.W. Wong, W.T. Wu, J. Yue, Two pore channel 2 (TPC2) inhibits autophagosomal-lysosomal fusion by alkalinizing lysosomal pH, J Biol Chem, 288 (2013) 24247-24263.
[70] H. Ivanova, T. Vervliet, L. Missiaen, J.B. Parys, H. De Smedt, G. Bultynck, Inositol 1,4,5-trisphosphate receptor-isoform diversity in cell death and survival, Biochim Biophys Acta, (2014).

Acknowledgements

We would like to thank C. Agnoletto for performing certain preliminary experiments. PP was supported by the Italian Association for Cancer Research (AIRC); Telethon (GGP11139B); local funds from the University of Ferrara; and the Italian Ministry of Education, University and Research (COFIN, FIRB, and Futuro in Ricerca). We also acknowledge Prof. Franco Tanzi, University of Pavia, for continuous support and collaboration.

Competing Financial Interests statement

The authors declare no competing financial interests.

Author contributions

DMP, VR, FD, SV, GGagliano, MT, GGuerra, LM, FM, DL performed experimental work and analyzed data; PP constructed and characterized the aequorin-based probes; AAG wrote the manuscript; FM and DM designed the study, analyzed all the data and wrote the manuscript.

Figure Legends

Figure 1. NAADP-induced membrane currents in HeLa cells. A, membrane currents were activated by dialysing HeLa cells with NAADP (10 nM) and monitored by applying conventional voltage ramps (-100 to +100 mV in 50 ms at 0.5 Hz) from a holding potential of 0 mV. Current amplitudes at -80 and + 80 mV were measured and plotted against the time to obtain the time course of current development. B, the I-V relationship of NAADP-evoked current was obtained when indicated by the asterisk in panel A. C, current oscillations were initiated by NAADP (10 nM) infusion in a fraction of cells and plotted as shown in panel A. D, I-V relationship of NAADP-induced current oscillations measured at the time indicated by the asterisk in panel C. E, dialysis of higher NAADP concentrations (50 and 100 μM) failed to induce any membrane current, thereby hinting at the desensitization of NAADP receptors. F, mean±SE of the amplitude of the current peak recorded at different doses of NAADP. G, the inclusion of NED-19 (10 μM) along with NAADP (10 nM) into the patch pipette prevented the onset of the bioelectrical signal. H, mean±SE of the amplitude of NAADP-evoked currents in the presence and absence of NED-19 (10 μM). NAADP was applied at 10 nM.

Figure 2. NAADP-induced membrane currents are mediated by TRPM4. A, NAADP-induced membrane currents were not inhibited by removal of external Ca^{2+} ($0Ca^{2+}$), but were reversibly abolished by replacing extracellular Na^{+} with N-methyl-D-glucamine ($0Na^{+}$). NAADP was applied at 10 nM. B, I-V relationships of NAADP-induced currents recorded from the cell displayed in panel A in the presence and absence of external Na^{+} ($0Na^{+}$). The I-V relationships were taken at the times indicated by the asterisks in panel A. C, membrane currents evoked by cytosolic dialysis of NAADP (10 nM) when intracellular K^{+} was replaced by NMDG. D, I-V relationship of the NAADP-evoked current recorded in the absence of intracellular K^{+} at the time indicated by the asterisk in panel C. E, NAADP-elicited membrane current under control conditions (Ctl) and in the presence of La^{3+} (50 μM), flufenamic acid (FFA; 20 μM), and 9-Phenanthrol (30 μM). F, mean±SE of the amplitude of NAADP-evoked currents under the designated treatments. G, NAADP-evoked currents in the absence and presence of 10 mM EGTA in the patch pipette to prevent a global increase in $[Ca^{2+}]_{i.}$

Figure 3. The disruption of acidic organelles suppresses NAADP-induced membrane currents. NAADP-induced membrane currents were hindered by pre-treating the cells with glycyl-L-phenylalanine-2-naphthylamide (GPN; 200 μM, 1 hour) (A and B), bafilomycin A1 (Baf A1; 100 nM, 1 hour) (C and D), and nigericin (50 μM, 20 min) (E and F). In each experiment, NAADP was

dyalised through the patch pipette at 10 nM. In Panels B, D and F, mean±SE of the amplitude of NAADP-evoked currents under the designated treatments.

Figure 4. The inhibition of Ca^{2+} release from the endoplasmic reticulum Ca^{2+} stores affects the bioelectrical response to NAADP. A, pre-incubating the cells with thapsigargin (2 μM, 1 hour) abrogated NAADP-induced membrane currents. B, the cytosolic infusion of heparin (1 mg/ml) along with NAADP (10 nM) through the patch pipette reduced and shortened NAADP-elicited current. C, the cytosolic dialysis of ryanodine (100 μM) or tetracaine (100 μM) abated the bioelectrical response to NAADP (10 nM). D, mean±SE of the amplitude of NAADP-evoked currents under the designated treatments.

Figure 5. Effect of GPN on EL and ER luminal Ca^{2+}. HeLa cells, were transfected with CathD-Aeq (A) or ER-Aeq (B), and 24 hour later were reconstituted with coelenterazine n in KRB solution supplied with 600 μM EGTA and 3 μM ionomycin at 4°C for 1 h. GPN, at indicated concentration, was added to the reconstitution solution for 20 min. After reconstitution, the cells were perfused with 2 mM Ca^{2+} (arrow) and the steady state Ca^{2+} levels in the EL (A) and ER (B) were measured. GPN was present in perfusion medium for the duration of the recording. The data are summarized in histograms and expressed as mean±SD of areas under the curves (AUC) normalized to control. *, $p < 0.05$; ***, $p < 0.001$.

Figure 6. Effect of bafilomycin A1 on EL and ER luminal Ca^{2+}. HeLa cells, transfected with CathD-Aeq (A) or ER-Aeq (B) and pre-treated with bafilomycin A1 (100 nM, 24 h) were reconstituted with 3 μM coelenterazine n in KRB supplied with 600 μM EGTA and 3 μM ionomycin at 4°C for 1 h. After reconstitution, the cells were perfused with 2 mM Ca^{2+} (arrow) and the steady state Ca^{2+} levels in the EL (A) and ER (B) lumen were measured. The data, summarized in histograms, expressed as mean±SD of areas under the curves (AUC) reported to control. ***, $p < 0.001$.

Figure 7. Effect of nigericin on EL and ER luminal Ca^{2+}. HeLa cells, expressing CathD-Aeq (A) or ER-Aeq (B) were reconstituted with 3 μM coelenterazine n in KRB supplied with 600 μM EGTA and 3 μM ionomycin at 4°C for 1 h. After reconstitution, the cells were perfused with 2 mM Ca^{2+} (arrow) and the steady state Ca^{2+} levels in the EL (A) and ER (B) lumen were measured. Indicated concentrations of nigericin were added to reconstitution solution 15-20 min prior to Ca^{2+} addition. The data, summarized in histograms, are expressed as mean±SD of areas under the curves

(AUC) reported to control. n indicates number of independent measurements per condition. ***, $p < 0.001$.

Figure 8. Effect of thapsigargin and tBHQ on EL and ER luminal Ca^{2+}. HeLa cells, transfected with CathD-Aeq (A) or ER-Aeq (B), and 24 hour later were reconstitured with coelenterazine n in KRB solution supplied with 600 μM EGTA and 3 μM ionomycin at 4°C for 1 h. After reconstitution, the cells were perfused with 2 mM Ca^{2+} (arrow) and the steady state Ca^{2+} levels in the EL (A) and ER (B) were measured. Thapsigargin (TG, 5 or 20 μM) or tBHQ (10 μM) were added to the cells 5 minutes before addition of Ca^{2+}. tBHQ was present in perfusate throughout all the experiment. The data are summarized in histograms and expressed as mean±SD of areas under the curves (AUC) normalized to control. *, $p < 0.05$; ***, $p < 0.001$.

Figure 9. Effect of bafilomycin, GPN and nigericin on tBHQ-sensitive Ca^{2+} compartments. HeLe cells were loaded with Fura-2/AM and transferred onto the stage of an epifluorescent microscope. A, the cells were perfused first with GPN (200 μM, 10 min, grey line and column) or with vehicle (DMSO)-containing (black line and column) Ca^{2+}-free KRB, after that perfusion was switched to the tBHQ-containing (20 μM) solution. B, the cells were first perfused with tBHQ (20 μM, 10 min), after which 200 μM GPN was added to the perfusion solution. C, HeLa cells were incubated overnight (O/N) with 100 nM bafilomycin A1 (BafA1, grey line and column). At the day of experiment, the cells were loaded with Fura-2/AM and perfused with Ca^{2+}-free KRB supplemented with 20 μM tBHQ. 100 nM BafA1 was present in all solutions. D, the cells were first perfused with nigericin (50 μM, 5 min, grey line and column) or with vehicle containing KRB (black line and column). After which, 20 μM tBHQ was added to perfusate. The data are summarized in histograms and expressed as mean±SD of areas under the curves (AUC) normalized to control. ***, $p < 0.001$.

Fig.1F

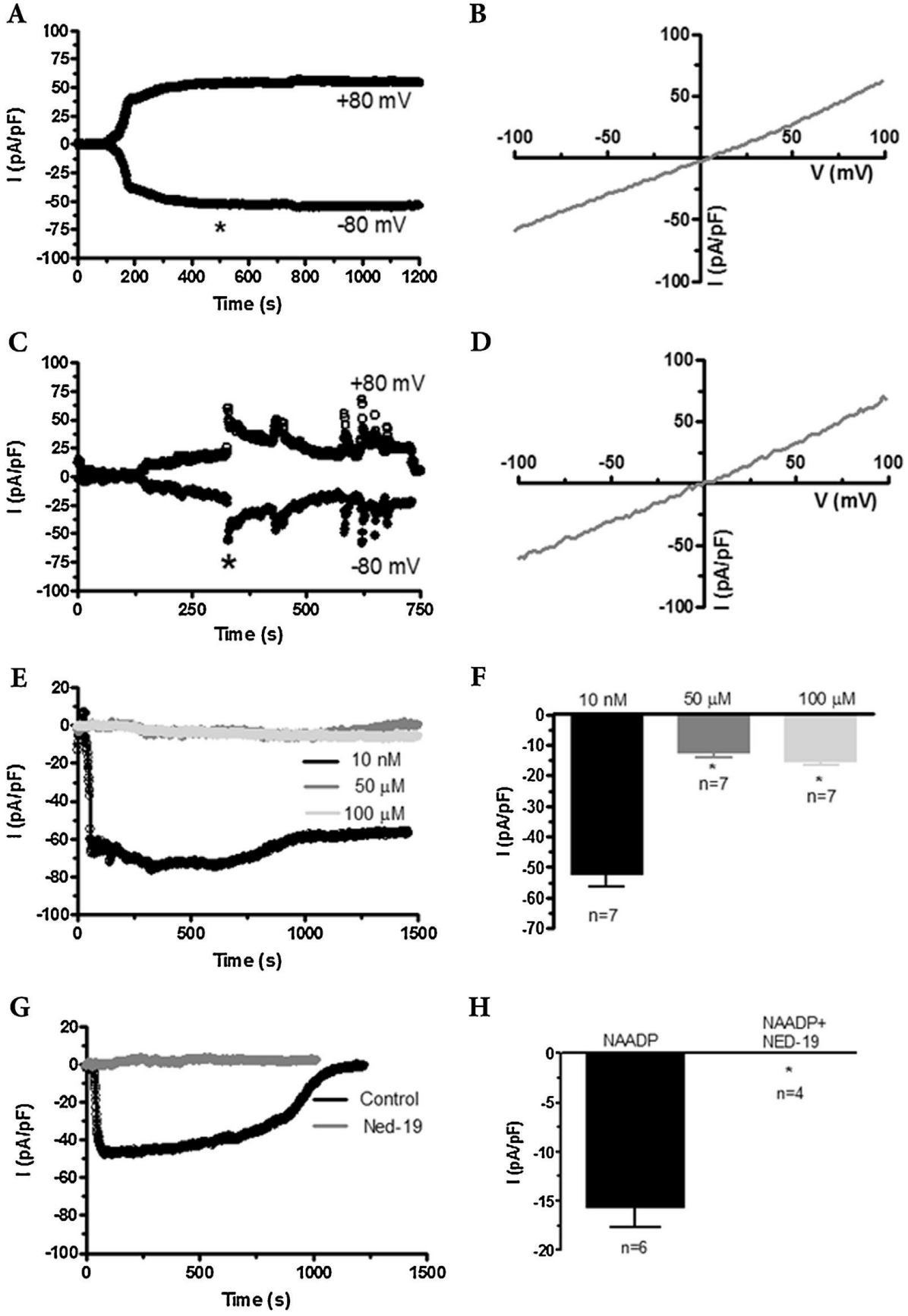
A
+80 mV
-80 mV
I (pA/pF)
Time (s)
B
V (mV)
I (pA/pF)
C
+80 mV
-80 mV
I (pA/pF)
Time (s)
D
V (mV)
I (pA/pF)
E
10 nM
50 µM
100 µM
I (pA/pF)
Time (s)
F
10 nM
50 µM
100 µM
n=7
n=7
n=7
I (pA/pF)
G
Control
Ned-19
I (pA/pF)
Time (s)
H
NAADP
NAADP+
NED-19
n=6
n=4
I (pA/pF)

Fig.1

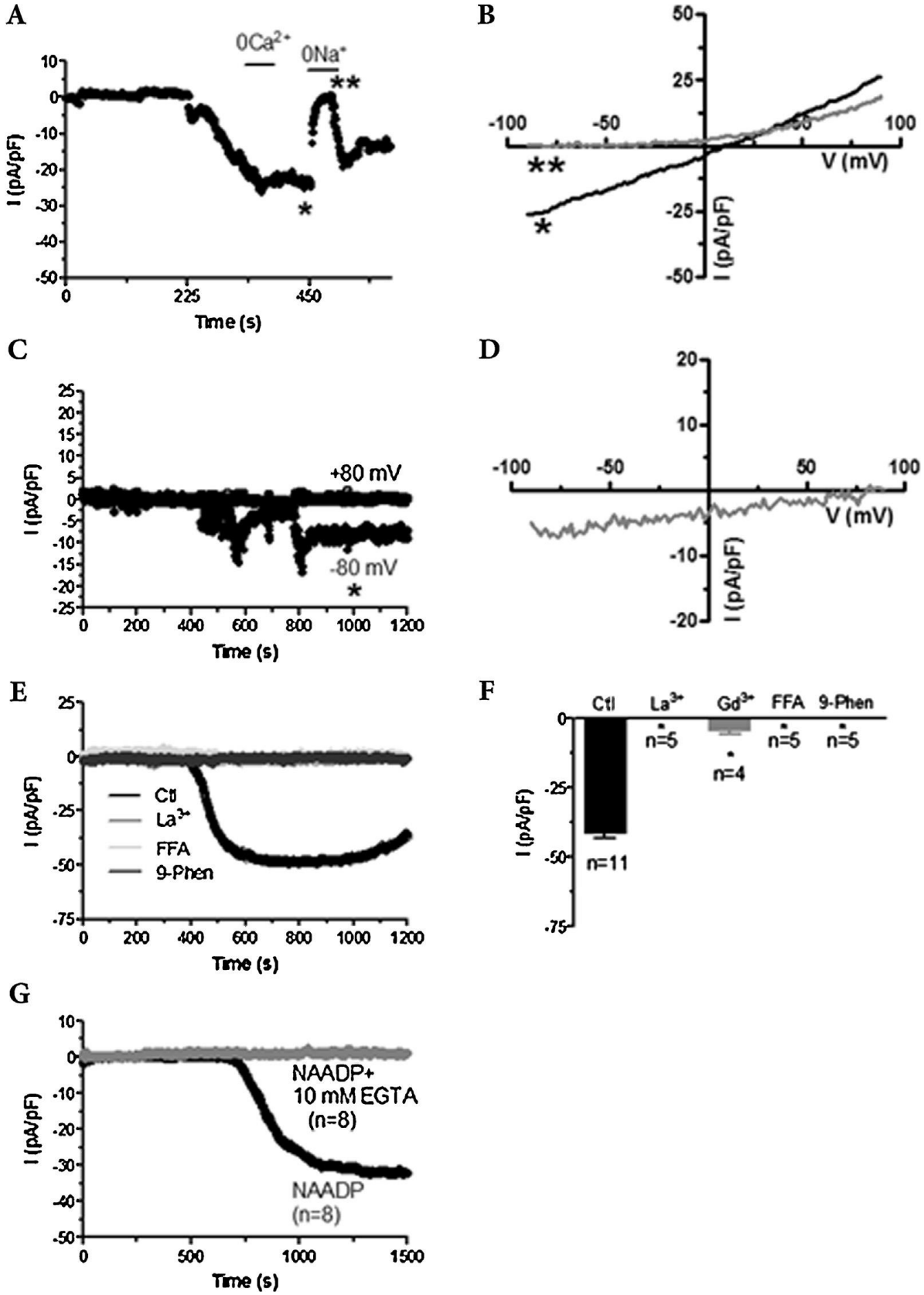
A
0Ca2+
0Na+
I (pA/pF)
Time (s)
B
V (mV)
I (pA/pF)
C
+80 mV
-80 mV
I (pA/pF)
Time (s)
D
V (mV)
I (pA/pF)
E
Ctl
La3+
FFA
9-Phen
I (pA/pF)
Time (s)
F
Ctl
La3+
Gd3+
FFA
9-Phen
n=11
n=5
n=4
n=5
n=5
I (pA/pF)
G
NAADP+
10 mM EGTA
(n=8)
NAADP
(n=8)
I (pA/pF)
Time (s)

Fig.2

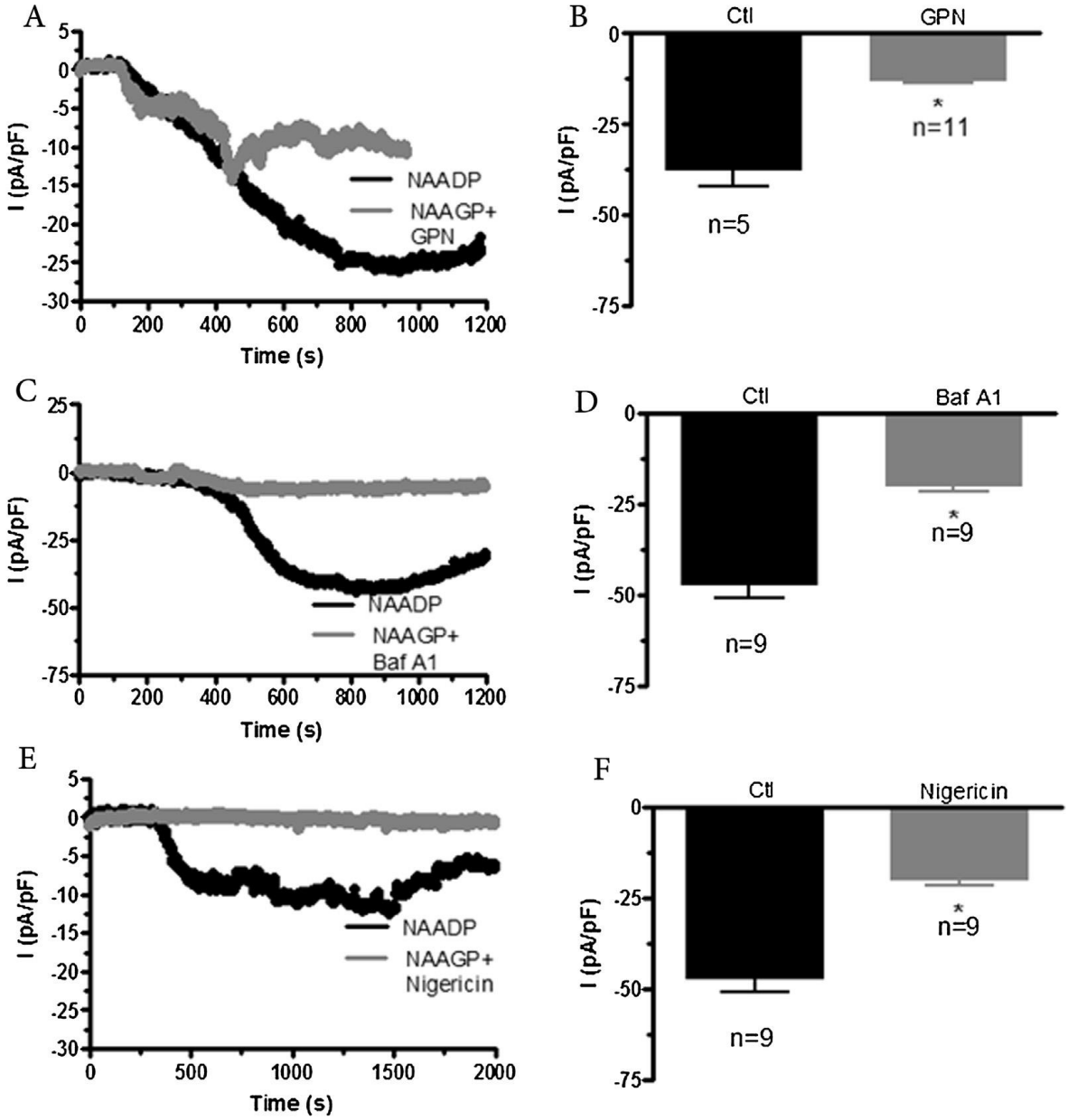
A
I (pA/pF)
Time (s)
NAADP
NAAGP+
GPN
B
Ctl
GPN
n=5
n=11
C
NAADP
NAAGP+
Baf A1
D
Ctl
Baf A1
n=9
n=9
E
NAADP
NAAGP+
Nigericin
F
Ctl
Nigericin
n=9
n=9

Fig.3

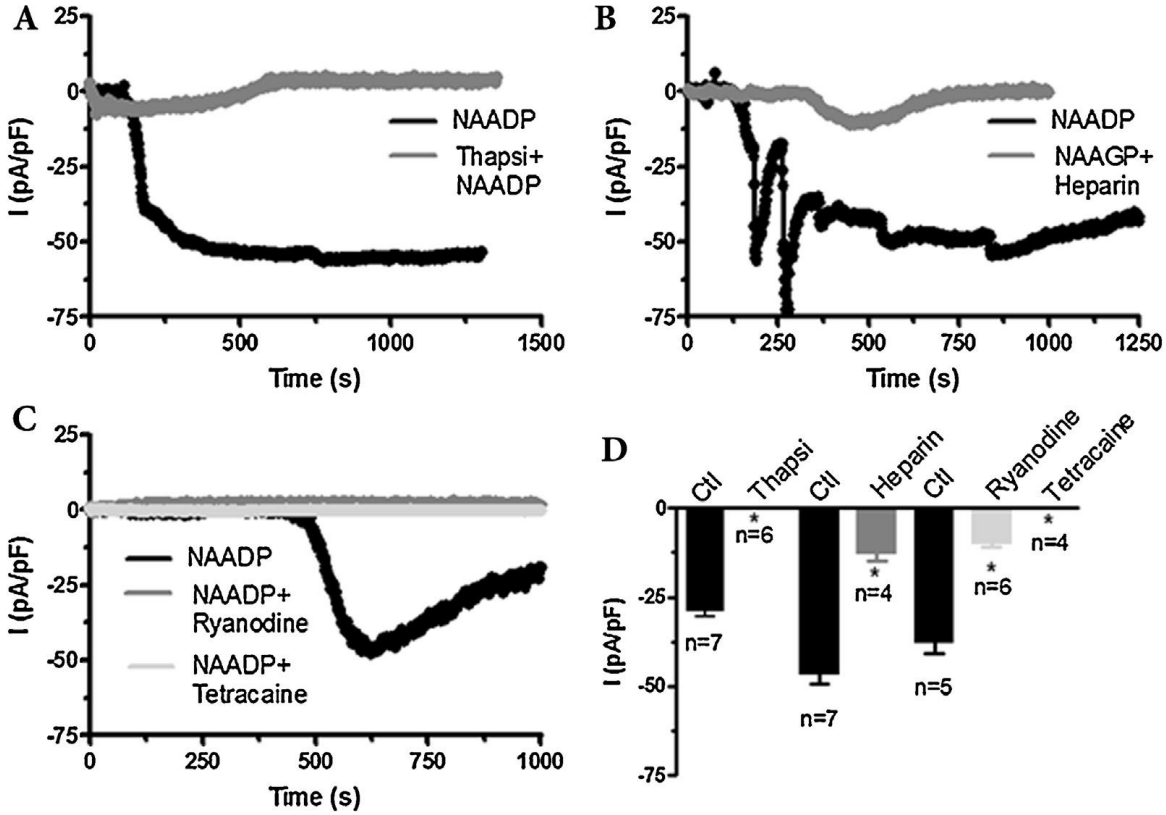
A
B
C
D
I (pA/pF)
Time (s)
NAADP
Thapsi+
NAADP
NAAGP+
Heparin
NAADP+
Ryanodine
NAADP+
Tetracaine
Ctl
Thapsi
Heparin
Ryanodine
Tetracaine
n=7
n=6
n=4
n=5
n=6

Fig.4

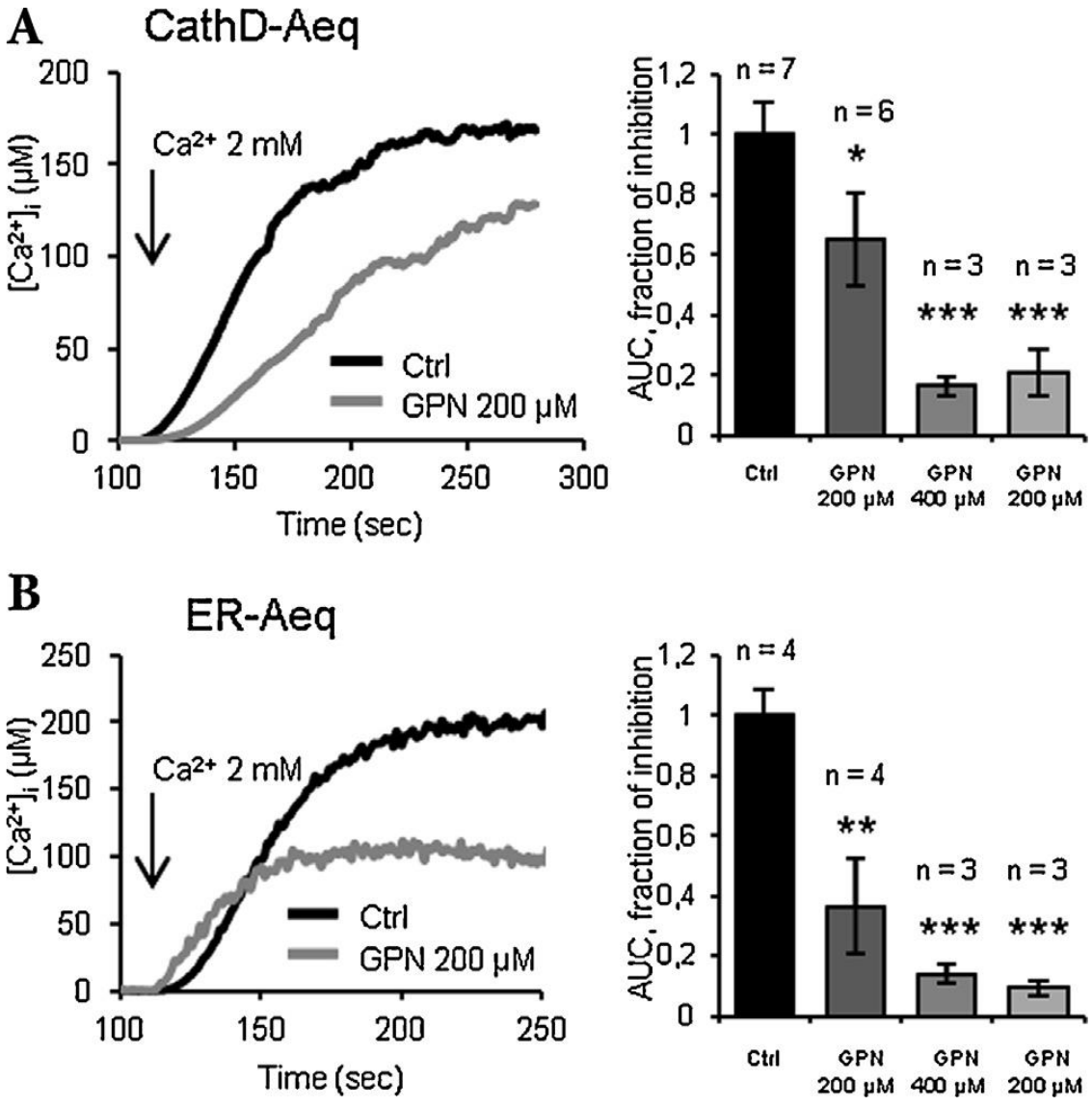
A
CathD-Aeq
[Ca2+]i (μM)
Ca2+ 2 mM
Ctrl
GPN 200 μM
Time (sec)
AUC, fraction of inhibition
n = 7
n = 6
n = 3
n = 3
*
***
***
Ctrl
GPN 200 μM
GPN 400 μM
GPN 200 μM
B
ER-Aeq
[Ca2+]i (μM)
Ca2+ 2 mM
Ctrl
GPN 200 μM
Time (sec)
AUC, fraction of inhibition
n = 4
n = 4
n = 3
n = 3
**
***
***
Ctrl
GPN 200 μM
GPN 400 μM
GPN 200 μM

Fig.5

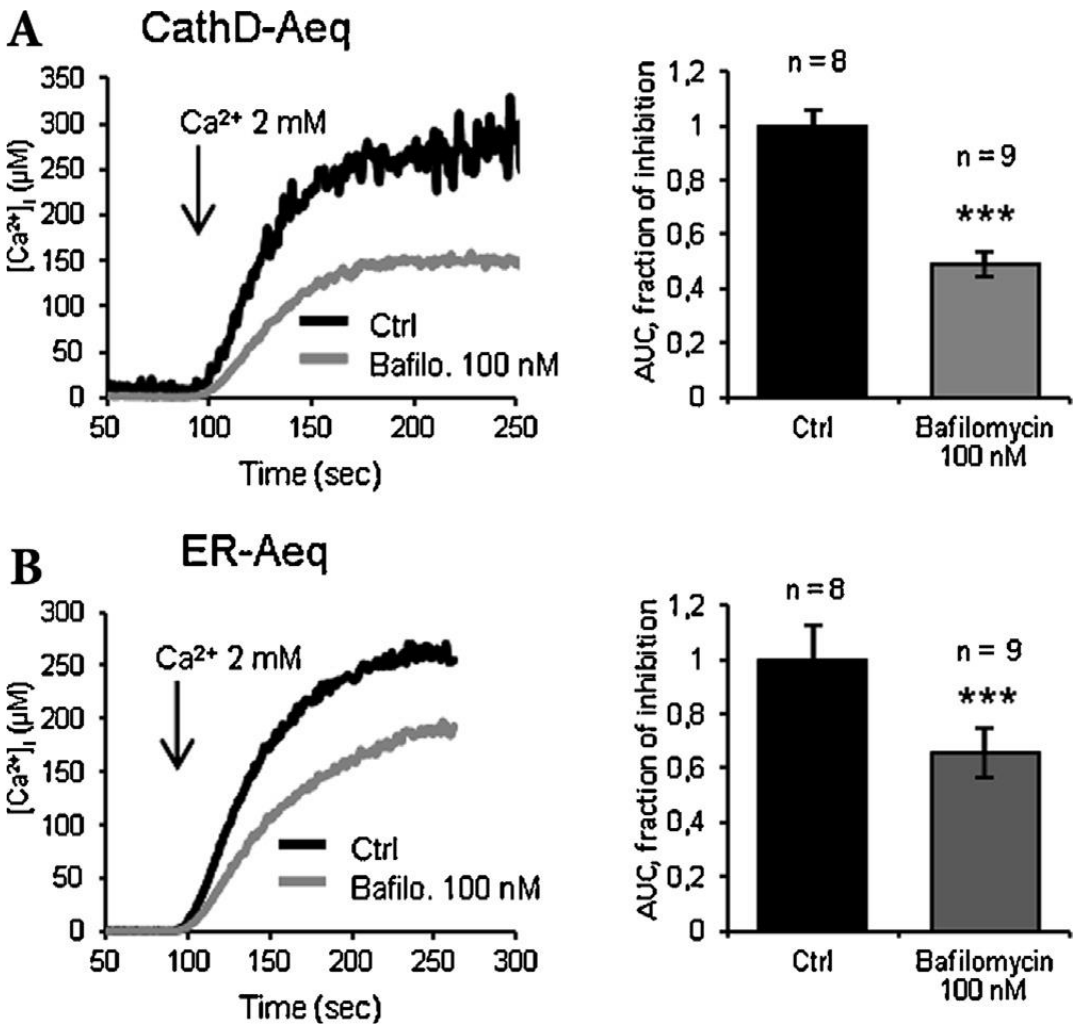
A
CathD-Aeq
Ca2+ 2 mM
[Ca2+]i (µM)
Time (sec)
Ctrl
Bafilo. 100 nM
AUC, fraction of inhibition
n = 8
n = 9
***
Ctrl
Bafilomycin 100 nM
B
ER-Aeq
Ca2+ 2 mM
[Ca2+]i (µM)
Time (sec)
Ctrl
Bafilo. 100 nM
AUC, fraction of inhibition
n = 8
n = 9
***
Ctrl
Bafilomycin 100 nM

Fig.6

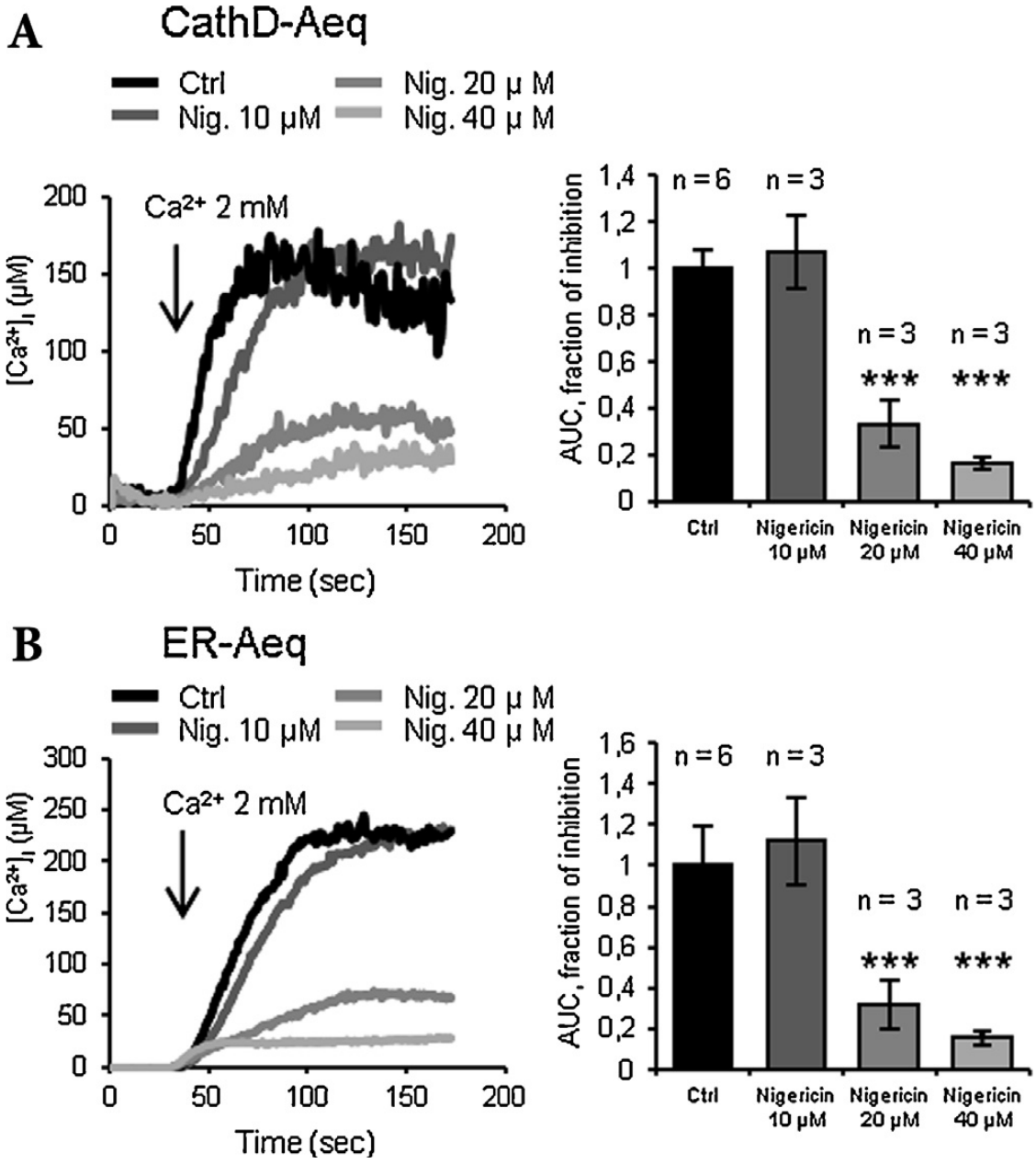
A
CathD-Aeq
Ctrl
Nig. 10 µM
Nig. 20 µ M
Nig. 40 µ M
Ca2+ 2 mM
[Ca2+]i (µM)
Time (sec)
AUC, fraction of inhibition
n = 6
n = 3
n = 3
n = 3
***
***
Ctrl
Nigericin 10 µM
Nigericin 20 µM
Nigericin 40 µM
B
ER-Aeq
Ctrl
Nig. 10 µM
Nig. 20 µ M
Nig. 40 µ M
Ca2+ 2 mM
[Ca2+]i (µM)
Time (sec)
AUC, fraction of inhibition
n = 6
n = 3
n = 3
n = 3
***
***
Ctrl
Nigericin 10 µM
Nigericin 20 µM
Nigericin 40 µM

Fig.7

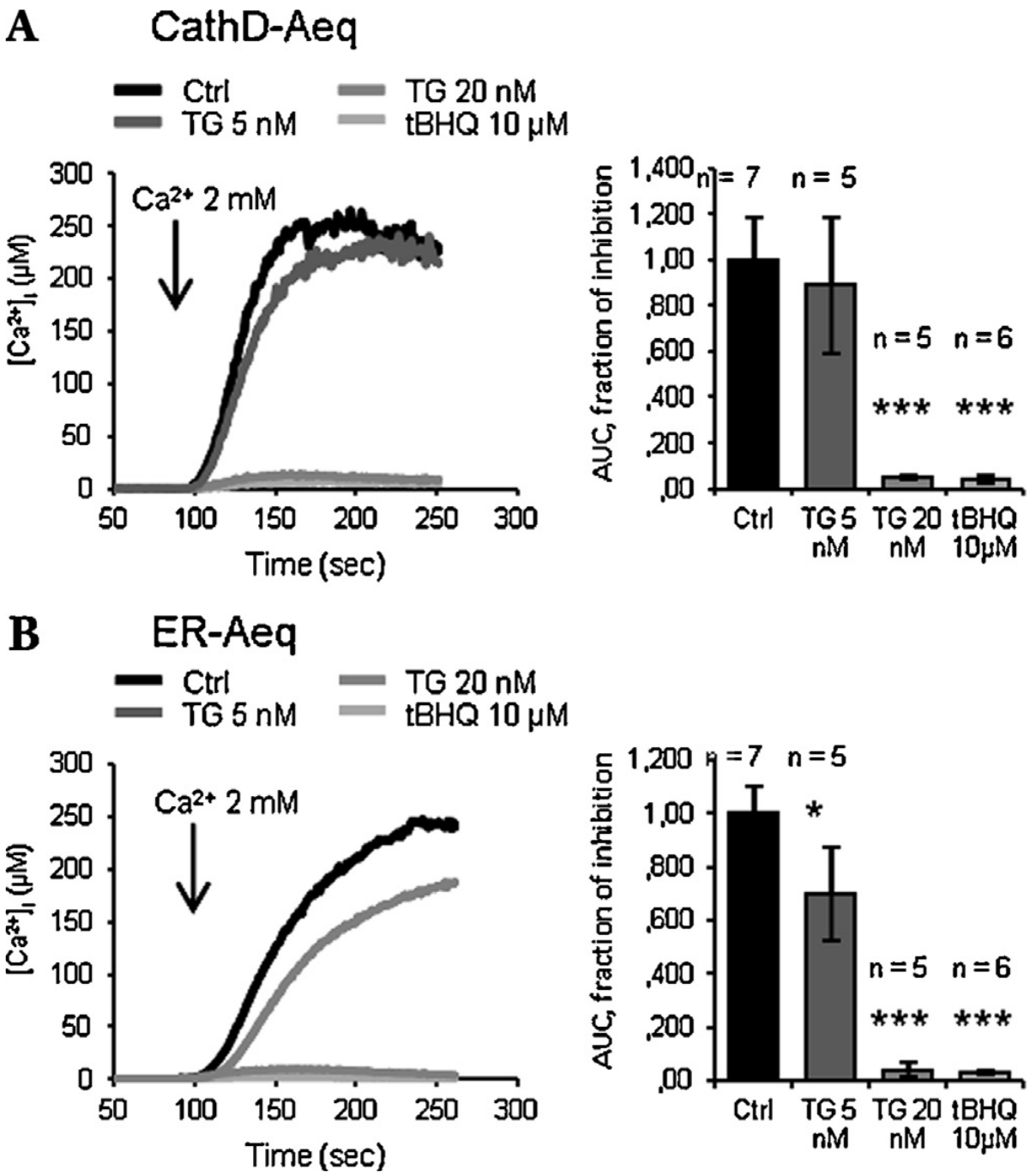
A
CathD-Aeq
Ctrl
TG 5 nM
TG 20 nM
tBHQ 10 µM
Ca2+ 2 mM
[Ca2+]i (µM)
Time (sec)
AUC, fraction of inhibition
n = 7
n = 5
n = 5
n = 6
***
***
Ctrl
TG 5 nM
TG 20 nM
tBHQ 10µM
B
ER-Aeq
Ctrl
TG 5 nM
TG 20 nM
tBHQ 10 µM
Ca2+ 2 mM
[Ca2+]i (µM)
Time (sec)
AUC, fraction of inhibition
n = 7
n = 5
*
n = 5
n = 6
***
***
Ctrl
TG 5 nM
TG 20 nM
tBHQ 10µM

Fig.8

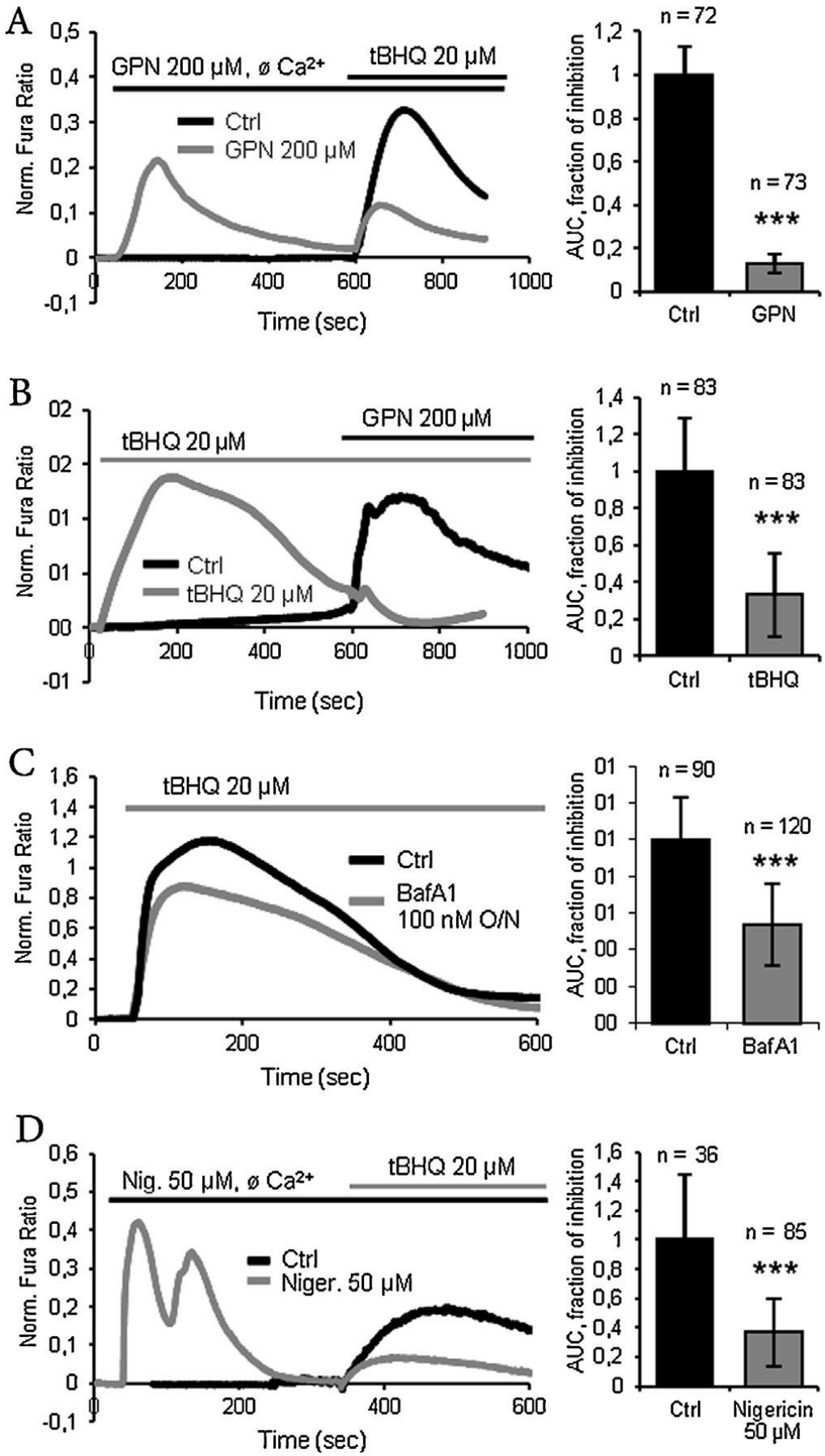
A
Norm. Fura Ratio
GPN 200 µM, ø Ca2+
tBHQ 20 µM
Ctrl
GPN 200 µM
Time (sec)
AUC, fraction of inhibition
n = 72
n = 73
***
Ctrl
GPN
B
Norm. Fura Ratio
tBHQ 20 µM
GPN 200 µM
Ctrl
tBHQ 20 µM
Time (sec)
AUC, fraction of inhibition
n = 83
n = 83
***
Ctrl
tBHQ
C
Norm. Fura Ratio
tBHQ 20 µM
Ctrl
BafA1
100 nM O/N
Time (sec)
AUC, fraction of inhibition
n = 90
n = 120
***
Ctrl
BafA1
D
Norm. Fura Ratio
Nig. 50 µM, ø Ca2+
tBHQ 20 µM
Ctrl
Niger. 50 µM
Time (sec)
AUC, fraction of inhibition
n = 36
n = 85
***
Ctrl
Nigericin
50 µM

Fig.9